Part 2

SHAPE ANALYSIS

The problem of shape analysis for long time has been given constant attention in computer vision. As a result, the field has been intensively developed over the past decades both in theoretical and applied domains. The shape of objects is a difficult concept. A shape parameter is a set function value of which does not depend on geometrical transformations such as translation, rotation, size changes and reflection. Currently three main directions in shape analysis can be observed: *functional approach*, *set theory approach* and *point description*. Each of them is based on certain mathematical ideas, that is, how the objects of which the shape is analyzed, are treated in mathematical terms. Here only two-dimensional objects or two-dimensional images of three-dimensional objects, which can be their projections or sections, are considered. It is assumed that the two-dimensional information is sufficient for a reasonable characterization. Further, it is always assumed that the objects are sets in the sense of mathematical set theory and that the sets are compact and closed in the topological sense. Such sets are called *figures*. Processing of figures in sense of set theory leads to the set theoretic approach of shape analysis. Two different topics fractal theory and simple geometrical rations, are discussed in this chapter. An important method for characterizing figures is the representation of their contours by functions. Such representation is possible in many ways and it results in the functional approach of shape analysis. Having such contour functions many results of functional analysis and differential geometry can be applied to study the shape. An extensive overview of this approach is given in this chapter. The third direction in shape analysis (which is not discussed here) is related to the replacement of figures by a few points which usually lie on the contour and are defined by some geometrical properties or have a certain physical meaning. Such 'point fields' can be analyzed, for example, by statistical methods.

2.1. Functional approach

The function description methods of figures are appropriate for many applications because of their advantages over other methods such as

i) effective data reduction: frequently only a few coefficients of the approximation functions are needed for a rather precise form description;
ii) a convenient description of complex forms;
iii) an intuitive characterization of many form properties.

Of course, there are some disadvantages: the necessary choice of a reference point taken as the origin, which often appears to be arbitrary; the complicated formulae for functions and characteristics even for simple figures, etc. Functional representation is 'in the middle' between the set-based and point-based ones. In practice it means that all information available when dealing with set- or point-description methods, is also available dealing with functional approach. Moreover, it is possible to regenerate a set representation as well as to derive a point-based representation of a figure from its functional representation. All these features make functional approach practical and frequently used in shape analysis.

2.1.1. Contour functions

The contour of a figure can be described by a function. There are two basic ideas to introduce such a function:

i) the contour of a figure can be symmetric with respect to a line; than the orthogonal distance of the contour point from the symmetry line as a function of position on the symmetry line can be considered as a contour function;
ii) the contour function may be periodic, the contour itself can be considered as a periodic function; assuming that the contour has some desirable properties such as star-shapedness or convexity, a relatively simple contour functions, such as the radius-vector or support functions, can be introduced, otherwise more complex contour functions, such as the tangent-angle function or the contour itself, can be considered as contour functions.

Cross-section functions for symmetric figures

It is natural to describe the form of a symmetric figure by the cross-section function [2.1.1], the half-breadth at x. Suppose that a symmetric figure is oriented in such a way that its symmetry axis coincides with the x-axis of the coordinate system. Only one-half of the

figure is considered and for each point the coordinates $(x, q_X(x))$ are obtained where $q_X(x)$ is the half-breadth at x (Fig. 2.1.1a).

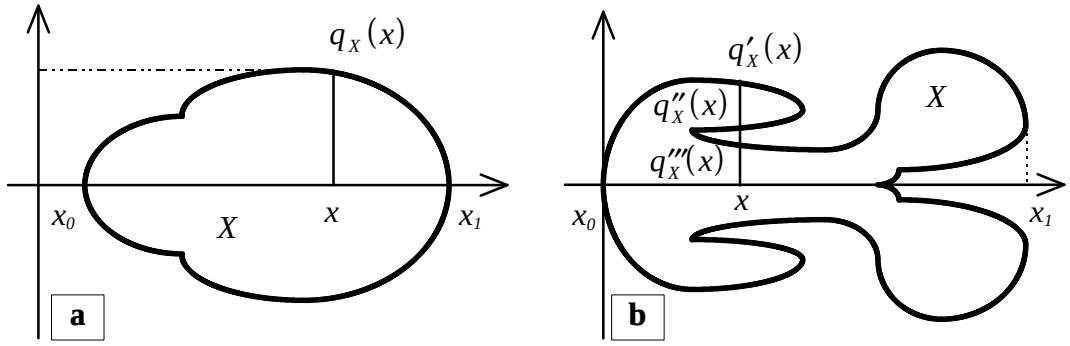

Fig. 2.1.1. a) definition of the cross-section function for a symmetric figure; **b)** problems with the cross-section functions occur if there is more than one contour point on the line through x orthogonal to the symmetry axis.

Problems occur if there is more than one contour point on the line through x orthogonal to the symmetry axis (Fig. 2.1.1b). This ambiguity can be removed by choosing the mean distance as the function value, or the outer contour point or by smoothing the contour. Of course, these simplifications may destroy essential features of the contour and in this case it is better not to use cross-section functions at all. An example of a symmetric figure and its cross-section function is given in Fig. 2.1.2.

For the shape analysis problem it is important to know some properties of the cross-section function. The cross-section function $q_X(x)$ of a figure X

1) is invariant under translation: $q_{X+v}(x) = q_X(x)$ where $X + v$ is X translated by a vector v;
2) depends from changes of the size of the figure X: $q_{\lambda X}(x) = \lambda q_X(x)$ where λX is the figure X zoomed by a factor λ;
3) does not depend on the orientation of the figure X;
4) is in the general case not invariant under reflection;
5) is not periodic;
6) from the fact that a figure X is a subset of a figure Y ($X \subset Y$) follows that $q_X(x) \le q_Y(x)$.

Some geometrical figure parameters, such as the perimeter $P(X)$ and area $A(X)$ of the figure X, can be obtained by integration of the cross-section function $q_X(x)$:

$$P(X) = 2\int_{x_0}^{x_1} \sqrt{1 + q'^2_X(x)}\,dx \quad \text{and} \quad A(X) = 2\int_{x_0}^{x_1} q_X(x)\,dx .$$

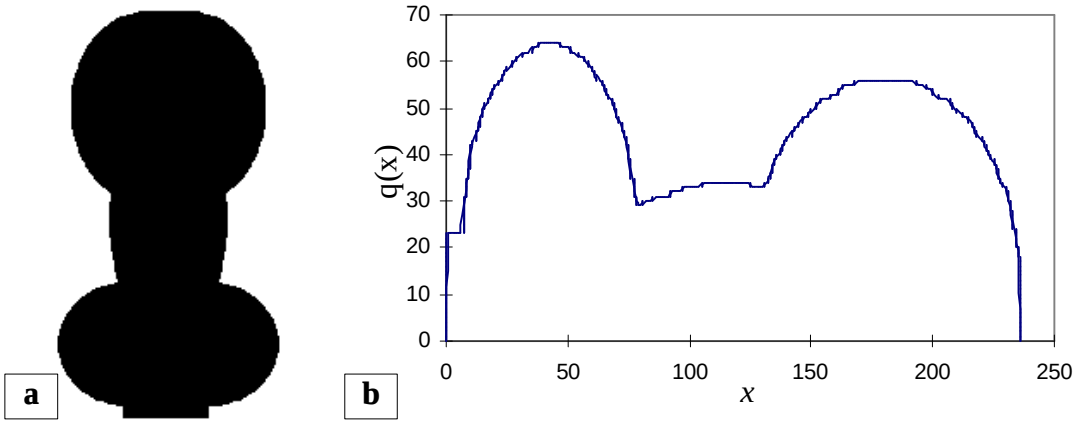

Fig. 2.1.2. a) a symmetric figure X ; **b)** cross-section function $q_X(x)$ of the figure X .

Radius-vector functions

Frequently the contour of a figure is described by the *radius-vector function* [2.1.1-2.1.3] defined in the following way. A reference point O in the interior of the figure X is selected. It is usually the center of gravity, or the center of the smallest disc which completely contains the figure or a physically important point. Next, the appropriate reference line l crossing the reference point O is chosen, usually parallel to the x- or y-axes. The radius-vector function $r_X(\varphi)$ is then the distance from the reference point O to the contour in the direction of the φ-ray where $0 \le \varphi \le 2\pi$ (Fig. 2.1.3a).

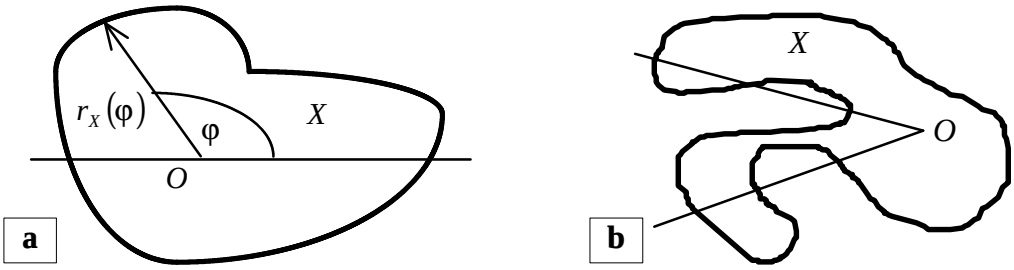

Fig. 2.1.3. a) radius-vector function; **b)** problems with the radius-vector function occur if the figure is not star-shaped.

It is necessary, however, that the figure is star-shaped with respect to O; that is, for any contour point p the whole line segment from O to p lies within the figure. In this case the radius-vector function completely characterizes the figure: if $r_X(\varphi)$ is given, than the figure can be completely reconstructed. If the star-shapedness is violated only by small irregularities in the contour it is possible to recover it by smoothing. In the general case, however,

description by the radius-vector function is not suitable for non-star-shaped figures. An examples of a star-shaped figure and its radius-vector function is given in Fig. 2.1.4.

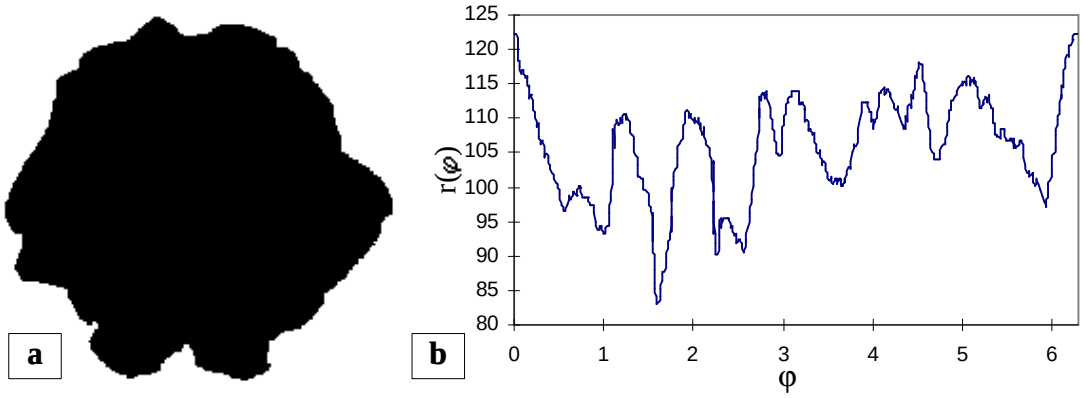

Fig. 2.1.4. a) a start-shaped figure X ; **b)** radius-vector function $r_X(\varphi)$ of the figure X. The center of gravity of the figure was used as the origin to generate the radius-vector function.

For the shape analysis problem it is important to know how the radius-vector function $r_X(\varphi)$ of a star-shaped figure X depends on basic geometrical transformations such as *translation*, *size changes*, *rotation* and *reflection* and which other properties it has. The radius-vector function $r_X(\varphi)$ of a star-shaped figure X

1) is invariant under translation: $r_{X+v}(\varphi) = r_X(\varphi)$ where $X+v$ is X translated by a vector v;
2) depends on the changes of the size of the figure X : $r_{\lambda X}(\varphi) = \lambda r_X(\varphi)$ where λX is the figure X zoomed by a factor λ ;
3) depends on the orientation of the figure X : $r_X(\varphi) = r_Y(\varphi - \alpha)$ where Y is the figure X rotated by an angle α ;
4) is not invariant under reflection;
5) is periodic with the period 2π : $r_X(\varphi + 2\pi) = r_X(\varphi)$;
6) from the fact that a start-shaped figure X is a subset of a star-shaped figure Y ($X \subset Y$) follows that $r_X(\varphi) \le r_Y(\varphi)$.

The map $X \to r_X$ transforms star-shaped figures into elements of a function space; radius-vector functions of star-shaped figures are continuous in φ ; consequently they can be embedded in the Banach space $C[0,\ 2\pi]$ of all continuous functions on $[0,\ 2\pi]$.

When the radius-vector function $r_X(\varphi)$ of a star-shaped figure X is available some geometrical figure parameters can be obtained. Integrating of $r_X(\varphi)$ yields the perimeter

$P(X)$, area $A(X)$ and mean radius-vector length $\bar{r}_X$:

$$P(X) = \int_0^{2\pi} \sqrt{r_X^2(\varphi) + r_X'^2(\varphi)}\, d\varphi \,,\; A(X) = \frac{1}{2}\int_0^{2\pi} r_X^2(\varphi)\, d\varphi \text{ and } \bar{r}_X = \frac{1}{2\pi}\int_0^{2\pi} r_X(\varphi)\, d\varphi \,.$$

A quantitative index of differences between radius-vector functions of different figures may be obtained by determination of the average squared deviation of the radius-vector function from a circle of equal area. This 'roughness coefficient' may be defined as:

$$R'_X = \frac{1}{2\pi}\int_0^{2\pi} r_X^2(\varphi)\, d\varphi - \left(\frac{1}{2\pi}\int_0^{2\pi} r_X(\varphi)\, d\varphi\right)^2 .$$

Support functions

For a figure X the *support function* [2.1.1] is defined as follows. Let g_φ be an oriented line through the origin O with direction φ ($0 \le \varphi \le 2\pi$) and let $g_\varphi^\perp$ be the line orthogonal to g_φ so that the figure X lies completely in the half-plane determined by $g_\varphi^\perp$ with $g_\varphi^\perp \cap X \neq \varnothing$, which is opposite to the direction of g_φ (Fig. 2.1.5a). The absolute value of the support function equals to the distance from O to $g_\varphi^\perp$ and the support function $s_X(\varphi)$ is negative if the figure lies behind $g_\varphi^\perp$ as seen from the origin. If O is an element of the figure X than $s_X(\varphi) \ge 0$ for all φ.

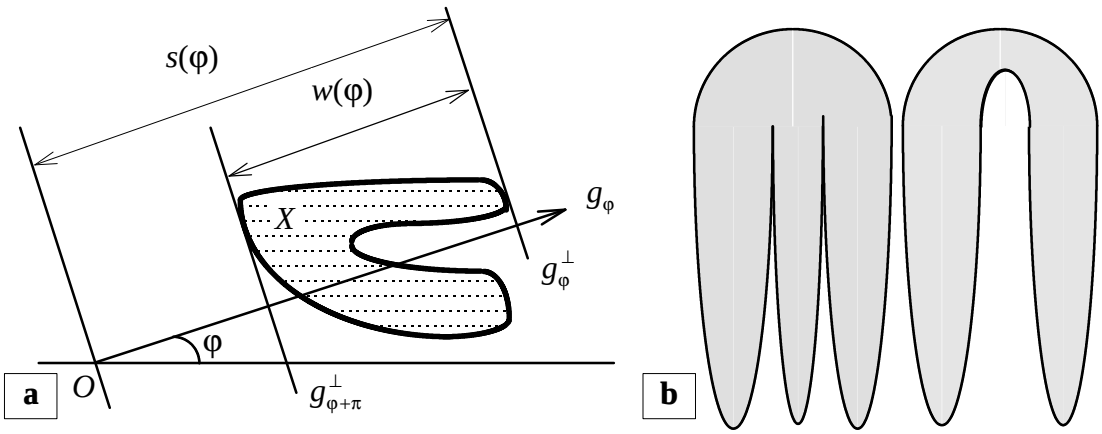

Fig. 2.1.5. a) definition of the support function $s_X(\varphi)$ and the width function $w_X(\varphi)$ of the figure X ; **b)** both figures have the same support functions.

An equation to calculate the support function $s_X(\varphi)$ can be written taking into account the *normal equation* of a line. Consider the closed contour of a figure X in Euclidean space. Let the perimeter of the figure X be L. Every point $(x_X(l),\ y_X(l))$ of the contour of X can

thus be identified with a number l, with $0 \le l \le L$, run through anti-clockwise. Than the support function $s_X(\varphi)$ can be calculated as $s_X(\varphi) = \max_{0 \le l \le L} \{x_X(l)\cos\varphi + y_X(l)\sin\varphi\}$.

It is obvious that there exist different non-convex figures with the same support function (Fig. 2.1.5b). In contrast, convex figures are uniquely determined by their support functions. An example of a convex figure and its support function is given in Fig. 2.1.6.

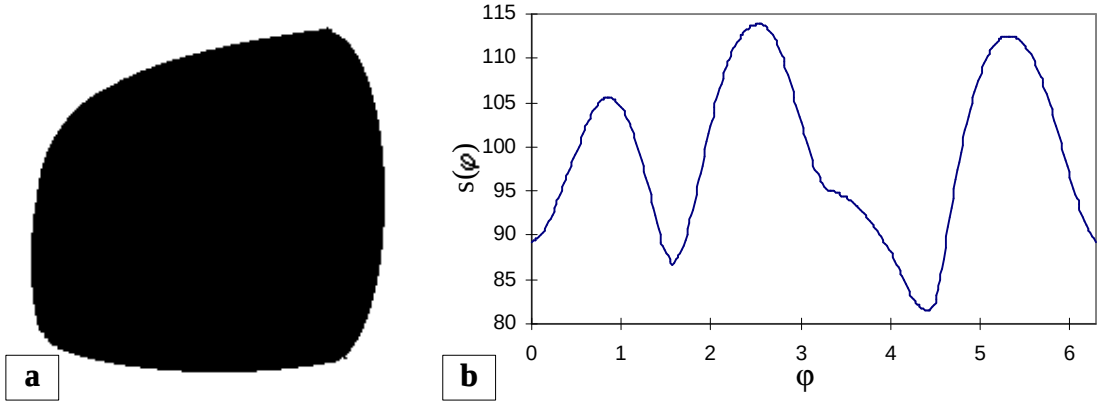

Fig. 2.1.6. a) a convex figure X ; **b)** support function $s_X(\varphi)$ of the figure X. The center of gravity of the figure was used as the origin to generate the support function.

For the shape analysis problem it is important to know some properties of the support function. The support function $s_X(\varphi)$ of a convex figure X

1) is, in general, not invariant under translation except when O is an element of the figure X ;
2) depends on changes of the size of the figure X : $s_{\lambda X}(\varphi) = \lambda s_X(\varphi)$ where λX is the figure X zoomed by a factor λ ;
3) depends on the orientation of the figure X : $s_X(\varphi) = s_Y(\varphi - \alpha)$ where Y is the figure X rotated by an angle α ;
4) is not invariant under reflection;
5) is periodic with the period 2π : $s_X(\varphi + 2\pi) = s_X(\varphi)$;
6) from the fact that a convex figure X is a subset of a convex figure Y ($X \subset Y$) follows that $s_X(\varphi) \le s_Y(\varphi)$;
7) if a convex figure X is symmetric then $s_X(\varphi) = s_X(\varphi + \pi)$.

The map $X \to s_X$ transforms convex figures into elements of a function space; support functions of convex figures can be embedded in the Banach space $C[0,\ 2\pi]$ of all continuous functions on $[0,\ 2\pi]$.

If a convex figure X has a smooth boundary, then its support function $s_X(\varphi)$ determines

the curvature. The curvature radius $\rho_X(\varphi)$ of the figure X corresponding to φ is related to the support function $s_X(\varphi)$ as $\rho_X(\varphi) = s_X(\varphi) + s_X''(\varphi)$ where $0 \le \varphi \le 2\pi$.

Having support function $s_X(\varphi)$ of a convex figure X its perimeter $P(X)$ and area $A(X)$ satisfy

$$P(X) = \int_0^{2\pi} s_X(\varphi)d\varphi \text{ and } A(X) = \frac{1}{2}\int_0^{2\pi} s_X(\varphi)\left(s_X(\varphi) + s_X''(\varphi)\right)d\varphi .$$

Width function

The so-called *width function* [2.1.1] $w_X(\varphi)$ (Fig. 2.1.5a) is closely related to the support function of the figure X: $w_X(\varphi) = s_X(\varphi) + s_X(\varphi + \pi)$ where $0 \le \varphi \le \pi$. Physically $w_X(\varphi)$ is the breadth of the figure in the direction φ. For form analysis the width function has the advantage that it is invariant with respect to translation. But rotation changes the width function. In general, the width function does not describe the form of a figure uniquely even if the figure is convex. An example of a figure and its width function is given in Fig. 2.1.7.

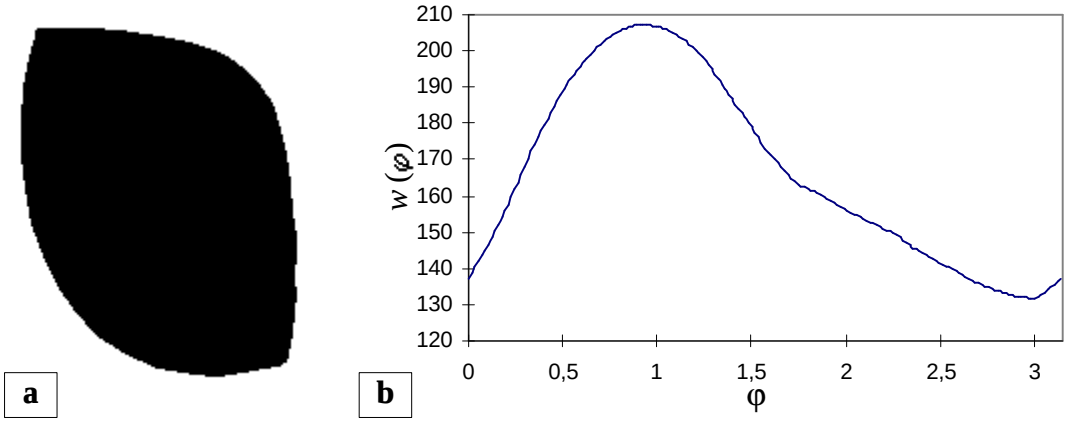

Fig. 2.1.7. a) a figure X ; **b)** width function $w_X(\varphi)$ of the figure X.

Having the width function $w_X(\varphi)$ of the figure X some contour parameters can be obtained. The perimeter $P(X)$ of the figure can be yielded as

$$P(X) = \frac{1}{2}\int_0^{2\pi} w_X(\varphi)d\varphi ,$$

however the area is not uniquely determined by the width function.

Contour parametric and contour complex functions

Consider the closed contour of a figure X in Euclidean space. Let the perimeter of the figure X be L. Every point p_l of the contour of X can thus be identified with a number l, with $0 \le l \le L$, run through anti-clockwise. Their coordinates are $\left(x_X(l),\ y_X(l)\right)$. A point moving along the contour in the anti-clock-wise direction generates a function which can be represented parametrically as $c_X(l) = \left(x_X(l),\ y_X(l)\right)$. A contour parametrization in which the contour is parametrized by its arc length is called a *natural parametrization*.

Now consider the closed contour of a figure X in polar coordinates. Every point p_l of the contour of X has polar coordinates $\left(d_X(l),\ \theta_X(l)\right)$. A point moving along the contour in the anti-clockwise direction generates a function which can be represented parametrically as $\tau_X(l) = \left(d_X(l),\ \theta_X(l)\right)$.

Finally, consider the closed contour of a figure X in a complex plane. Every point p_l of the contour of X has its complex coordinates $z_X(l) = x_X(l) + iy_X(l)$. A point moving along the contour in the anti-clockwise direction generates a complex function $z_X(l)$ [2.1.4-2.1.7].

It is important to note that these three different contour functions are identical; the only difference is that they represent the same thing for different coordinate systems. Having one contour function representation, the two other can be easily obtained:

$$z_X(l) = x_X(l) + iy_X(l),\ c_X(l) = \left(\mathrm{Re}\, z_X(l),\ \mathrm{Im}\, z_X(l)\right),$$
$$\tau_X(l) = \left(\left|z_X(l)\right|,\ \arg z_X(l)\right),\ c_X(l) = \left(\left|d_X(l)\right|\cos\theta_X(l),\ \left|d_X(l)\right|\sin\theta_X(l)\right).$$

Examples of the contour parametric functions are given in Fig. 2.1.8.

When one of these functions of a figure X is available some geometrical figure parameters can be calculated. The perimeter $P(X)$ of the contour is

$$P(X) = \int_0^L \sqrt{x'^2_X(l) + y'^2_X(l)}\, dl\,.$$

The *oriented figure area* $A(X)$ is given by the well-known differential geometry formula

$$A(X) = \frac{1}{2}\oint_{(C)} \left(x_X(l)\frac{dy_X(l)}{dl} - y_X(l)\frac{dx_X(l)}{dl} \right) dl$$

where $A(X)$ is positive or negative depending on where the figure is located when it is traced on the contour C - from the left or right side, respectively. Equations of the *tangent* and *normal* at a point $\left(x_X(l),\ y_X(l)\right)$ of a figure X are:

$$\frac{y - y_X(l)}{y'_X(l)} = \frac{x - x_X(l)}{x'_X(l)} \text{ and } x'_X(l)\left(x - x_X(l)\right) + y'_X(l)\left(y - y_X(l)\right) = 0\,.$$

The *curvature* $\kappa_X(l)$ and the *curvature radius* $\rho_X(l)$ at a point $\left(x_X(l),\ y_X(l)\right)$ can be calculated as

$$\kappa_X(l) = \frac{x'_X(l)y''_X(l) - x''_X(l)y'_X(l)}{\left(x'^2_X(l) + y'^2_X(l)\right)^{3/2}} \text{ and } \rho_X(l) = \frac{1}{\left|\kappa_X(l)\right|}.$$

The *coordinates* $(x_k,\ y_k)$ *of* the *center of curvature* at a point $\left(x_X(l),\ y_X(l)\right)$ are defined as

$$x_k = x_X(l) - \frac{y'_X(l)\left(x'^2_X(l) + y'^2_X(l)\right)}{x'_X(l)y''_X(l) - y'_X(l)x''_X(l)} \text{ and } y_k = y_X(l) + \frac{x'_X(l)\left(x'^2_X(l) + y'^2_X(l)\right)}{x'_X(l)y''_X(l) - y'_X(l)x''_X(l)}.$$

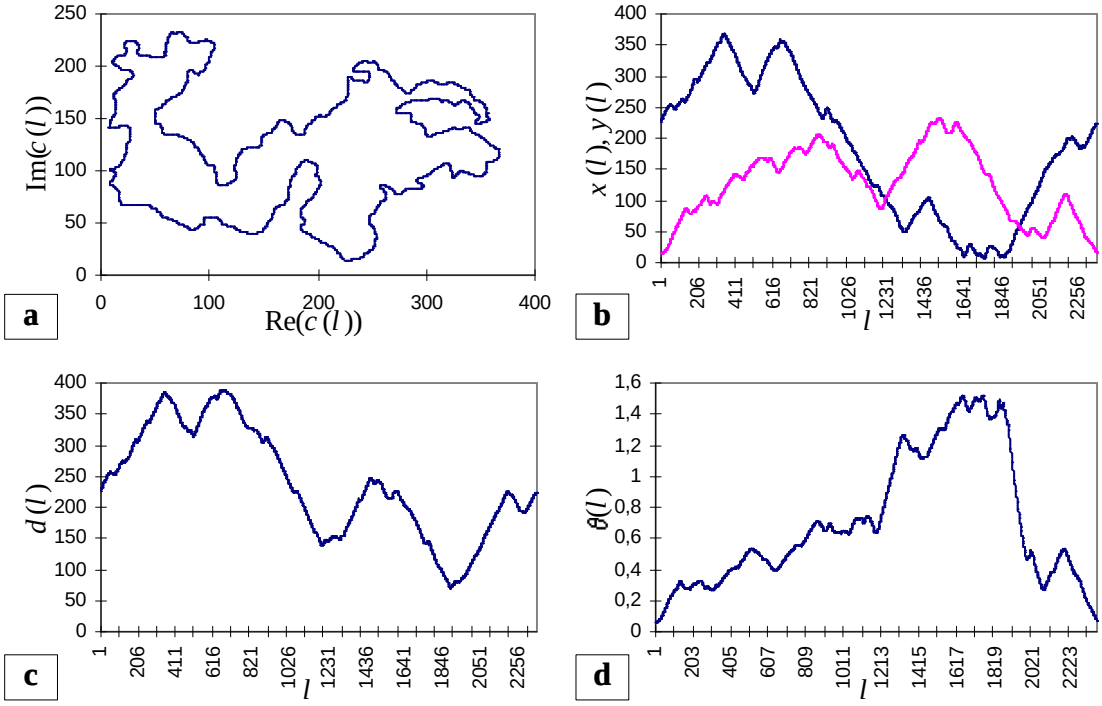

Fig. 2.1.8. a) a complex function $z_X(l)$ of a figure X; **b)** parametric function $c_X(l) = \left(x_X(l),\ y_X(l)\right)$ of the figure X; **c, d)** parametric function $\tau_X(l) = \left(d_X(l),\ \theta_X(l)\right)$ of the figure X.

Some properties of the contour complex and parametric functions are recalled. The functions

1) are not invariant under translation of the figure X;
2) are not invariant under changes of the size of the figure X;
3) depend on the orientation of the figure X;

4) are not invariant under reflection of the figure X ;
5) are periodic with the period L .

However, these functions are very attractive in such fields of shape analysis as Fourier and wavelets analyses and they are the basis to obtain any other contour functions.

For shape analysis it is sometimes helpful to normalize these functions in such a way that the perimeter length is eliminated and the functions are defined on $[0,\ 2\pi]$. It can be done in the following way. The perimeter is normalized by defining $t = 2\pi l L^{-1}$ and the functions are normalized as

$$c_X^*(t) = c_X\left(tL(2\pi)^{-1}\right),\ \tau_X^*(t) = \tau_X\left(tL(2\pi)^{-1}\right) \text{ and } z_X^*(t) = z_X\left(tL(2\pi)^{-1}\right).$$

Tangent-angle function

Often the tangent angle at different points of the contour is used for the description of a figure [2.1.1, 2.1.8]. It is assumed that the contour of the considered figure is piecewise-smooth so that a tangent may not exist at a finite number of points.

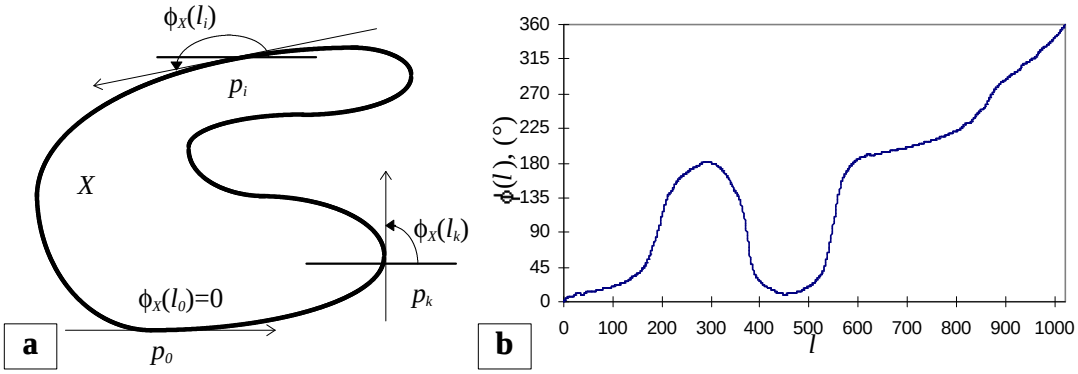

Fig. 2.1.9. a, b) definition of the tangent-angle function $\phi_X(l)$ of figure X .

Let the perimeter of the figure X be L . Every point p_l of the contour of X can thus be identified with a number l , with $0 \le l \le L$, run through anti-clockwise. A pointer is places at p_0 so that its zero position coincides with the tangent direction at p_0 . If the pointer moves on the contour then it changes its direction in such a way that it is always in the direction of the tangent, where its orientation is given by the direction of the movement. The angle given by the pointer direction at p_l is denoted $\phi_X(l)$ where $\phi_X(0) = 0$ and $\phi_X(L) = 2\pi$ (Fig. 2.1.9). The function $\phi_X(l)$ is called the *tangent-angle function.*

For shape analysis it is helpful to normalize the function $\phi_X(l)$ in such a way that the

perimeter length is eliminated and the function is defined on $[0,\ 2\pi]$ like the radius-vector and support functions. In practice it is done as follows. The perimeter is normalized by defining $t = 2\pi l L^{-1}$ and $\phi_X(l)$ is normalized as

$$\phi_X^*(t) = \phi\left(Lt(2\pi)^{-1}\right) + t$$

where $0 \le t \le 2\pi$ and $\phi_X^*(0) = \phi_X^*(2\pi) = 0$. An examples of a figure and its normalized tangent angle function is given in Fig. 2.1.10.

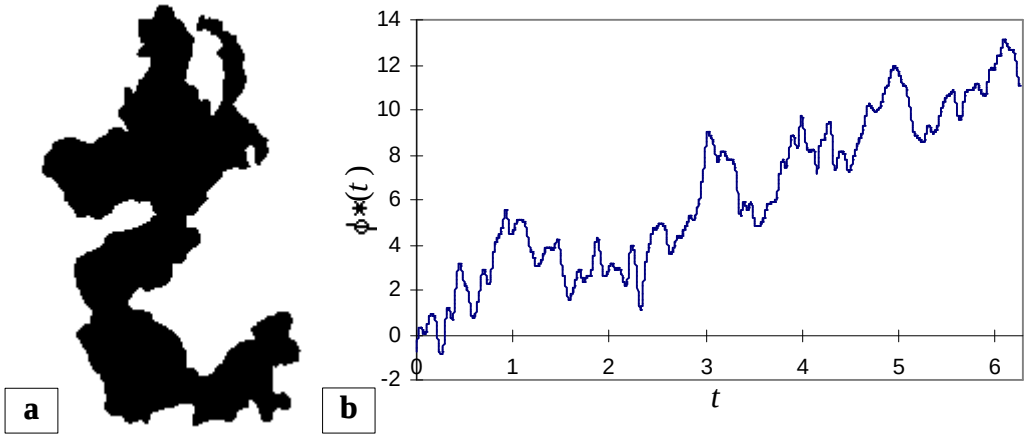

Fig. 2.1.10. a) a figure X ; **b)** the normalized tangent-angle function $\phi_X^*(t)$ of the figure.

Some properties of the tangent-angle function are recalled. The normalized tangent-angle function $\phi_X^*(t)$ of a figure X

1) is invariant under translation: $\phi_{X+v}^*(t) = \phi_X^*(t)$ where $X + v$ is X translated by a vector v;
2) is invariant under changes of the size of the figure X : $\phi_{\lambda X}^*(t) = \phi_X^*(t)$ where λX is the figure X zoomed by a factor λ ;
3) does not depend on the orientation of the figure X ;
4) is not invariant under reflection;
5) is periodic with the period 2π : $\phi_X^*(t + 2\pi) = \phi_X^*(t)$.

The map $X \to \phi_X^*$ transforms figures into elements of a function space, but the normalized tangent-direction functions of figures in the general case are not continuos.

An important discrete version of the tangent-angle function for the case of digital contours is *chain encoding*. The result of chain encoding is the direction from a point of the contour to its nearest neighbor point along the contour in the anti-clockwise direction as function of the index of the contour point. Such function is a sequence of numbers 0, 1, ..., 7 which

correspond to the angles 0º, 45º, 90º, ..., 115º.

The intrinsic equation of the contour

The *intrinsic equation* of the contour is a logical extension of the tangent-angle function. It is defined to be the curvature as function of the contour arc length [2.1.9-2.1.12]. Such representation of the contour plays a key role in differential geometry. The importance of this approach is immediately clear when looking at the *fundamental theorem* in the analysis of curves: *if two single-valued continuous functions are given then there exists one and only one planar curve, determined but for its position on the plane, for which one of the given functions is the arc length (measured from an appropriate point on the curve) and other is the curvature.*

Three different definitions of the curvature can be given:

i) *path based continuous curvature:*

$$\kappa_X(l) = \frac{x'_X(l)y''_X(l) - x''_X(l)y'_X(l)}{\left(x'^2_X(l) + y'^2_X(l)\right)^{3/2}};$$

i) *orientation based continuous curvature*: $\kappa_X(l) = \phi'_X(l)$;

ii) *osculating circle based continuous curvature*:

$$\kappa_X(l) = \begin{cases} +\dfrac{1}{\rho_X(l)} & \text{if contour is locally convex} \\ -\dfrac{1}{\rho_X(l)} & \text{if contour is locally concave} \end{cases}.$$

The definitions are equivalent in the continuous case but not in the discrete case. Different methods of curvature estimation are based on one of these definitions. An example of a curvature function is given in Fig. 2.1.11.

Curvature function has the same properties as those mentioned for the tangent-angle function. Some geometrical contour features are related to the contour curvature function $\kappa_X(l)$. Thus, the *corners* are locations on the contour where the curvature $\kappa_X(l)$ becomes unbounded. In practice, a corner is declared whenever $|\kappa_X(l)|$ assumes a large value. Another attribute associated with the curvature is the *bending energy*:

$$E_X = \frac{1}{L}\int_0^L |\kappa_X(l)|^2 \, dl \, .$$

The definition of the *detrended function* $\hat{\theta}_X(l)$ of the contour is closely related to its curvature:

$$\hat{\theta}_X(l) = \int_o^l \kappa(p)dp - \frac{2\pi l}{L}.$$

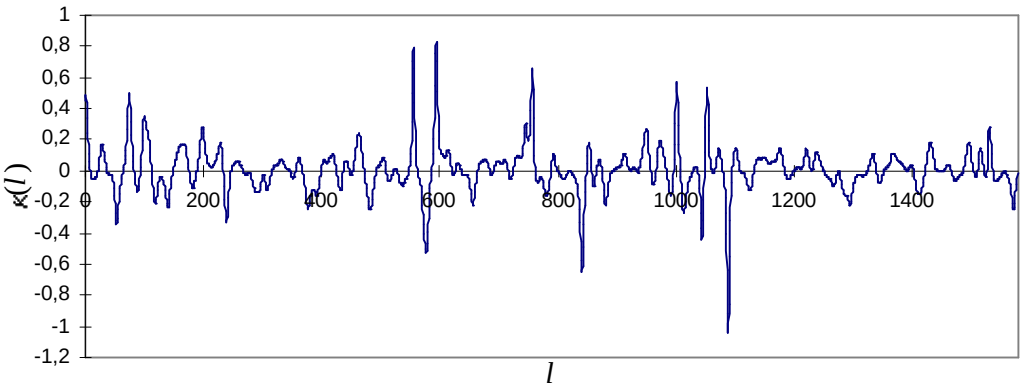

Fig. 2.1.11. Curvature function $\kappa_X(l)$ of the figure shown in Fig. 2.1.10a.

Concluding remarks on contour functions

The contour functions, described above, have certain advantages and disadvantages for shape analysis. Application of the cross-section function is limited only to symmetric figures. The radius-vector function requires the figure to be star-shaped whereas for the support function convexity is desirable. The tangent-angle function, the contour curvature and contour complex functions as well as the contour parametric functions can be applied to any contours. All discussed functions depend on the choice of a reference point, they have complex relations to the basic geometrical transformations such as translation, rotation, size changes and reflection. All of them, except the cross-section and width functions, are or can be defined on $[0,\ 2\pi]$.

Generally speaking, the entire mathematical theory of functions as well as the differential and computational geometry can be applied to analyze the contour functions. In practice, however, only some ideas are used. In addition the contour of a figure or its contour function can be considered as a realization of a random process. In this case the theory of stochastic models and the statistical analysis are appropriate tools to be used in shape analysis.

2.1.2. Application of contour functions to shape analysis

The largest area of applications of contour functions and what makes them so attractive for shape analysis is not just the possibility to calculate some simple geometrical parameters of figures such as the perimeter and area, but the potentiality to expand them into time series and the possibility to approximate them by simpler functions which can then be easily analyzed.

Before describing how these contour functions can be used for shape analysis a few important remarks should be made. For the theoretical considerations it is always assumed that a contour function $f(x)$ is continuous and continuously differentiable, with the expectation of a finite number of points. However, in practice of image processing, continuos contours of figures are never available but only their discrete approximations at some nodes. Consequently contour functions are also determined as a sequence of interpolation nodes x_i and of corresponding function values $f(x_i)$ where $i = 1, 2, \ldots N$. Thus, instead of a contour function $f(x)$, its discrete numerical version $f(x_i)$ is considered. Usually it is given as lists of numbers. One of consequences of such replacement is that the integration and differentiation of these functions are not continuous anymore and are performed by methods of numerical analysis.

Invariant contour function parameters

Some simple quantities of contour functions can be determined [2.1.1]. They can be used when the radius-vector function, the width function, the tangent-vector function, the contour curvature or the contour parametric functions are available.

The *mean value* of the contour function $f(x)$ and its numerical approximation are given by

$$\bar{f} = \frac{1}{2\pi}\int_0^{2\pi} f(x)dx \approx \frac{1}{N}\sum_{i=1}^{N} f(x_i).$$

The mean value $\bar{f}$ of the contour function $f(x)$ is a size parameter except in the case of the tangent-vector, the contour curvature and the contour parametric functions. In the latter case it reveals the center of gravity of the contour.

The *variance* of the contour function $f(x)$ is given by

$$\sigma^2(f) = \frac{1}{2\pi}\int_0^{2\pi}\left[f(x) - \bar{f}\right]^2 dx \approx \frac{1}{N}\sum_{i=1}^{N}\left(f(x_i) - \bar{f}\right)^2 .$$

The variance $\sigma^2(f)$ of the contour function $f(x)$ is a size, shape and roundness characteristic. The *variance of the derivative* of the contour function $f(x)$ is given by

$$\sigma^2(f') = \frac{1}{2\pi}\int_0^{2\pi} f'^2(x)dx \approx \frac{1}{N}\sum_{i=1}^{N}\left(\frac{f(x_{i-2}) - 8f(x_{i-1}) + 8f(x_{i+1}) - f(x_{i+2})}{12\Delta}\right)^2$$

where $\Delta = 2\pi N^{-1}$, $x_{-1} = x_{N-1}$, $x_0 = x_N$, $x_{N+1} = x_1$, $x_{N+2} = x_2$. The variance $\sigma^2(f')$ of the derivative describes local properties such as roundness and texture variations.

The *covariance function* of the contour function $f(x)$ is given by

$$\chi_f(\varphi)=\frac{1}{2\pi}\int_0^{2\pi}\left[f(x)-\bar{f}\right]\left[f(x+\varphi)-\bar{f}\right]dx,\ \chi_f(k\Delta)=\frac{1}{N}\sum_{i=1}^{N}\left[f(x_i)-\bar{f}\right]\left[f(x_{i+k})-\bar{f}\right]$$

where $0\le\varphi\le 2\pi$, $f(2\pi+x)=f(x)$, $x_{N+k}=x_k$. The covariance $\chi_f(\varphi)$ describes some aspects of local and global form fluctuations. The normalized function $\chi_f(\varphi)\chi_f^{-1}(0)$ characterizes the shape of the figure.

The quantities $\bar{f}$ and $\sigma^2(f)$ can be interpreted as mean and variance corresponding to a distribution function $F_f(x)$, defined as follows:

$$F_f(x)=\frac{1}{2\pi}L\left(\left\{\varphi:\ f(\varphi)\le 0;\ 0\le\varphi\le 2\pi\right\}\right),\ x\ge 0$$

where L denotes the Lebesgue measure of R^1 which is the length for a regular set in R^1. The distribution function $F_f(x)$ of the contour function $f(x)$ is a size, shape and roundness characteristic.

Line moments and invariants

A very useful and practical set of shape descriptors is based on the theory of moments [2.1.4, 2.1.13] which, for the case of the figure contour, can be introduced as follows [2.1.14, 2.1.15]. Consider the parametric representation $c_X(l)$ of the contour C of a figure X. The *line moments* along the contour are given by

$$m_{p,q}^{(1)}=\oint_{(C)}x_X^p(l)y_X^q(l)\delta(l)dl$$

where $\delta(l)$ is a linear density of the contour which for simplicity can be taken as 1. The number $p+q$ is called the *order* of the moment. The line moments usefulness for shape analysis follows from the *moment uniqueness theorem*: *the infinite set of the line moments uniquely determines the contour, and vice-versa*.

In practice, calculation of the linear moments can be performed by simple summation:

$$m_{p,q}^{(1)}\approx\sum_{i=1}^{N}\left(x_X(l_i)\right)^p\left(y_X(l_i)\right)^q$$

where N is the number of available points of the contour C. This formula is different when only an approximation of the contour by a polygon is available. If the contour is approximated by an n-side polygon with vertexes (x_i, y_i) where $i=1,2,\ldots n$, each line segment u_i can be parameterized by $y=a_ix+y_i-a_ix_i$ where $x_i\le x\le x_{i+1}$ and $a_i=(y_{i+1}-y_i)/(x_{i+1}-x_i)$ is the slope of the segment u_i. If the segment is vertical, the alternative parametrization should be used: $x=x_i$ where $y_i\le y\le y_{i+1}$. Then the following formula can be used to calculate the linear moments where C_k^q are binomial coefficients:

$$m_{p,q}^{(1)} \approx \sum_{i=1}^{n}\left[\begin{cases}\sqrt{1+a_i^2}\sum_{k=0}^{q}\left\{C_k^q a_i^k \left(y_i - a_i x_i\right)^{q-k} \dfrac{x_{i+1}^{p+k+1} - x_i^{p+k+1}}{p+k+1}\right\} & \text{if } u_i \text{ is not vertical} \\ x_i^p \dfrac{y_{i+1}^{q+1} - y_i^{q+1}}{q+1} & \text{if } u_i \text{ is vertical}\end{cases}\right].$$

The line moments are not invariant under the main geometrical transformations such as translation, rotation, scale change and reflection. However the *central moments* are invariant under translation. To obtain them the center of gravity of the contour C should be calculated which, actually, can be expressed through the zero- and first-order line moments:

$$\bar{x} = m_{1,0}^{(1)} \big/ m_{0,0}^{(1)} \text{ and } \bar{y} = m_{0,1}^{(1)} \big/ m_{0,0}^{(1)}.$$

Than the central moments are just

$$\mu_{p,q}^{(1)} = \oint_{(C)} \left(x_X(l) - \bar{x}\right)^p \left(y_X(l) - \bar{y}\right)^q \delta(l) dl.$$

The central moments up to the third order are also given by the following relations:

$$\mu_{0,0}^{(1)} = m_{0,0}^{(1)},\ \mu_{1,0}^{(1)} = \mu_{0,1}^{(1)} = 0,\ \mu_{2,0}^{(1)} = m_{2,0}^{(1)} - m_{0,0}^{(1)}\bar{x}^2,\ \mu_{1,1}^{(1)} = m_{1,1}^{(1)} - m_{0,0}^{(1)}\overline{xy},$$

$$\mu_{0,2}^{(1)} = m_{0,2}^{(1)} - m_{0,0}^{(1)}\bar{y}^2,\ \mu_{3,0}^{(1)} = m_{3,0}^{(1)} - 3m_{2,0}^{(1)}\bar{x} + 2m_{0,0}^{(1)}\bar{x}^3,$$

$$\mu_{2,1}^{(1)} = m_{2,1}^{(1)} - m_{2,0}^{(1)}\bar{y} - 2m_{1,1}^{(1)}\bar{x} + 2m_{0,0}^{(1)}\bar{x}^2\bar{y},\ \mu_{1,2}^{(1)} = m_{1,2}^{(1)} - m_{0,2}^{(1)}\bar{x} - 2m_{1,1}^{(1)}\bar{y} + 2m_{0,0}^{(1)}\overline{xy}^2 \text{ and}$$

$$\mu_{0,3}^{(1)} = m_{0,3}^{(1)} - 3m_{0,2}^{(1)}\bar{y} + 2m_{0,0}^{(1)}\bar{y}^3.$$

To obtain scaling invariant line moments, normalization by the contour length should be done which leads to

$$\eta_{p,q}^{(1)} = \mu_{p,q}^{(1)} \left(\mu_{0,0}^{(1)}\right)^{-(p+q+1)}.$$

Under rotation and reflection the moment-generation function will change. However, via the theory of algebraic invariants it is possible to find certain polynomials of the central line moments that remain unchanged under rotation and reflection. Some moment invariants are as follows:

i) for first-order moments: $\mu_{1,0}^{(1)} = \mu_{0,1}^{(1)} = 0$ are always invariant;

ii) for second-order moments the invariants are:

$$\phi_1^{(1)} = \mu_{2,0}^{(1)} + \mu_{0,2}^{(1)} \text{ and } \phi_2^{(1)} = \left(\mu_{2,0}^{(1)} - \mu_{0,2}^{(1)}\right)^2 + 4\left(\mu_{1,1}^{(1)}\right)^2;$$

iii) for third-order moments the invariants are:

$$\phi_5^{(1)} = \left(\mu_{3,0}^{(1)} - 3\mu_{1,2}^{(1)}\right)\left(\mu_{3,0}^{(1)} + \mu_{1,2}^{(1)}\right)\left(\left(\mu_{3,0}^{(1)} + \mu_{1,2}^{(1)}\right)^2 - 3\left(\mu_{2,1}^{(1)} + \mu_{0,3}^{(1)}\right)^2\right) +$$

$$+ \left(\mu_{0,3}^{(1)} - 3\mu_{2,1}^{(1)}\right)\left(\mu_{0,3}^{(1)} + \mu_{2,1}^{(1)}\right)\left(\left(\mu_{0,3}^{(1)} + \mu_{2,1}^{(1)}\right)^2 - 3\left(\mu_{1,2}^{(1)} + \mu_{3,0}^{(1)}\right)^2\right),$$

$$\phi_3^{(1)} = \left(\mu_{3,0}^{(1)} - 3\mu_{1,2}^{(1)}\right)^2 + \left(\mu_{0,3}^{(1)} - 3\mu_{2,1}^{(1)}\right)^2,\ \phi_4^{(1)} = \left(\mu_{3,0}^{(1)} + \mu_{1,2}^{(1)}\right)^2 + \left(\mu_{0,3}^{(1)} + \mu_{2,1}^{(1)}\right)^2 \text{ and}$$

$$\phi_6^{(1)} = \left(\mu_{2,0}^{(1)} - \mu_{0,2}^{(1)}\right)\left(\left(\mu_{3,0}^{(1)} + \mu_{1,2}^{(1)}\right)^2 - \left(\mu_{2,1}^{(1)} + \mu_{0,3}^{(1)}\right)^2\right) + 4\mu_{1,1}^{(1)}\left(\mu_{0,3}^{(1)} + \mu_{1,2}^{(1)}\right)\left(\mu_{0,3}^{(1)} + \mu_{2,1}^{(1)}\right);$$

iv) it has been shown [2.1.4] that for N^{th}-order moments where $N \geq 3$, there are $N+1$ absolute invariants, which remain unchanged under both reflection and rotation. A number of other invariants can be found that remain unchanged under rotation but change sign under reflection.

The relationship between invariant moments becomes more complicated for higher-order moments. However, moment invariants can be expressed more conveniently in terms of what are called *Zernike moments*. These moments are defined as the projections of a function of two variables on a class of Zernike polynomials.

Being invariant under linear coordinate transformations, the moment invariants are useful features in pattern recognition problems. Using N moments, a contour can be represented as a point in an N-dimensional vector space and the pattern recognition problem thus is converted into a standard decision theory problem, for which several approaches are available.

Several figure parameters are based on moments. The figure's *orientation* θ is the angle between the major axis of the figure and the x axis of the coordinate system in which the figure is considered:

$$\theta = \frac{1}{2}\arctan\left(\frac{2\mu_{1,1}^{(1)}}{\mu_{2,0}^{(1)} - \mu_{0,2}^{(1)}}\right).$$

Ones θ is known the *bounding rectangle* of the figure can be determined. The bounding rectangle is the smallest rectangle enclosing the object that is also aligned with its orientation. Its sides can be calculated as follows where $0 \leq l \leq L$:

$$h = \max\left\{x_X(l)\cos\theta + y_X(l)\sin\theta\right\} - \min\left\{x_X(l)\cos\theta + y_X(l)\sin\theta\right\},$$
$$w = \max\left\{-x_X(l)\sin\theta + y_X(l)\cos\theta\right\} - \min\left\{-x_X(l)\sin\theta + y_X(l)\cos\theta\right\}.$$

The *best-fit ellipse* of the figure can be also expressed in terms of the line moments. The best-fit ellipse is the ellipse whose second moments are equal that of the figure. Let a and b denote the length of semi-major and semi-minor axes of the best-fit ellipse. Then

$$a = \sqrt[4]{\frac{4}{\pi}}\sqrt[8]{\frac{\left(\mu(\theta)_{2,0}^{(1)}\right)^3}{\mu(\theta)_{0,2}^{(1)}}} \text{ and } b = \sqrt[4]{\frac{4}{\pi}}\sqrt[8]{\frac{\left(\mu(\theta)_{0,2}^{(1)}\right)^3}{\mu(\theta)_{2,0}^{(1)}}}$$

where

$$\mu(\theta)_{0,2}^{(1)} \text{ and } \mu(\theta)_{2,0}^{(1)}$$

are the second-order line moments of the contour C^* of the figure X^*, which is obtained by rotating the figure X by the angle $-\theta$.

The figure's *eccentricity* ε can be measured as:

$$\varepsilon = \sqrt{\frac{\mu_{0,2}^{(1)} \cos^2\theta + \mu_{2,0}^{(1)} \sin^2\theta - \mu_{1,1}^{(1)} \sin 2\theta}{\mu_{0,2}^{(1)} \sin^2\theta + \mu_{2,0}^{(1)} \cos^2\theta + \mu_{1,1}^{(1)} \cos 2\theta}} = \frac{\left(\mu_{2,0}^{(1)} - \mu_{0,2}^{(1)}\right)^2 + 4\mu_{1,1}^{(1)}}{A(X)}.$$

Finally the figure's contour *spread* S can be calculated in terms of the central moments as

$$S = \mu_{0,2}^{(1)} + \mu_{2,0}^{(1)}.$$

One of the advantages of the usage of the line moments in shape analysis is that neither the existence of an area nor a closed contour is required. The line moments can be calculated for an arbitrary collection of contour fragments.

Approximation of contour functions by other simple functions

Let there be given a sequence of interpolation nodes x_i and function values y_i where $i = 1, 2, \ldots n$. A suitable approximation by mathematically simple functions has to be determined. A common approach to solve this problem is the following. A function $F(x; c_1, c_2, ..., c_p)$ is chosen with parameters $c_1, c_2, ..., c_p$ which are to be determined in such a way that the sum of squares of deviations is minimized. A popular form of F is

$$F(x; c_1, c_2, ..., c_p) = \sum_{j=1}^{p} c_j g_j(x)$$

where $g_j(x)$ are certain functions, for example $g_j(x) = x^j$ (polynomial approximation) or $g_j(x) = \sin k_j x$ and $\cos k_j x$ (Fourier series approximation). In addition to these two variants, there is the possibility of choosing particular functions appropriate for a given problem. Approximation of the contour of a figure by an ellipse and linear piecewise approximation is described below. These two particular approximation methods are chosen because of their frequent use in shape analysis.

To approximate the contour of a figure by *an ellipse* several methods are available [2.1.1, 2.1.4]. The choice depends on the availability of various measures of the figure and on the deviations of the figures from an ideal ellipse. The following three methods are considered.

1) The best-fit ellipse can be expressed *in terms of the line moments.*
2) The D_{max} *method* involves measurement of area $A(X)$ of the figure X and determination of the line g that has the maximal intersection with X. If $d_{\max}$ is the length of $g \cap X$ which can be calculated as

$$d_{\max} = \max_{l_i, l_j \in X} \left\{ \sqrt{\left(x_X(l_i) - x_X(l_j)\right)^2 + \left(y_X(l_i) - y_X(l_i)\right)^2} \right\}$$

where the parametric representation of the contour C of a figure X is $c_X(l_i) = \left(x_X(l_i),\ y_X(l_i)\right)$, then $a = 0.5 d_{\max}$, $b = 2A(X)/(\pi d_{\max})$ and the slope of the line g gives the orientation of the ellipse.

3) The *area-perimeter* method is based on the following formulae:

$$a = \alpha + \sqrt{\alpha^2 - \frac{A(X)}{\pi}} \text{ and } b = \frac{A(X)}{\pi a} \text{ where } \alpha = \frac{1}{3}\left(\sqrt{\frac{A(X)}{\pi}} + \frac{P(X)}{\pi} \right).$$

Linear piecewise (polygonal) approximation [2.1.16] of the contour of a figure or contour functions (instead of both terms the word *curve* is used in the following text) is frequently used. It produces a polygon which closely resembles the original curve and the polygon vertexes are a representation of the curve. There are three basic methods to obtain such approximation.

1) *Resampling method* is based on an equivalent distance resampling of the curve starting from an arbitrary curve point. This is the most simple, but also an ineffective and wrong way of polygonal approximation when any information about the shape of the curve is not taken into account. With a large number of approximation nodes, it produces a smooth curve approximation.

2) In the *error criteria method* the quality of the fit of the polygon to the curve is measured in order to obtain a good polygonal approximation. Suppose that a curve from point A to B is approximated by the straight line segment AB. Let p_i denotes the curve points from point A to point B. The distance from p_i to the line AB is the approximation error of the curve AB by the line segment AB for a particular curve point p_i. This distance can be computed using the coordinates $\left(x_A, y_A\right)$, $\left(x_B, y_B\right)$ and $\left(x_{p_i}, y_{p_i}\right)$ of the points A, B and p_i, respectively, as

$$d_i = b\sqrt{\left(1 - \cos^2\alpha\right)} \text{ where } \cos\alpha = \left(b^2 + c^2 - a^2\right)/(2bc),$$

$$a = \sqrt{\left(x_{p_i} - x_B\right)^2 + \left(y_{p_i} - y_B\right)^2},\ b = \sqrt{\left(x_{p_i} - x_A\right)^2 + \left(y_{p_i} - y_A\right)^2} \text{ and}$$

$$c = \sqrt{\left(x_B - x_A\right)^2 + \left(y_B - y_A\right)^2}.$$

The *fitness criterion* can be either the mean square error E_2 or the maximal error $E_{\max}$:

$$E_2 = \sum_i d_i^2,\ E_{\max} = \max_i \{d_i\}.$$

The optimal linear piecewise approximation can be obtained by choosing the polygon vertexes in such a way that the overall approximation error is minimized. A solution of this problem is not a trivial and requires heavy computations. However, there exist two

approaches which are fast and relatively efficient in most cases. The *merge technique* works in the following way. Starting from the curve point p_0 and traversing the curve in the clockwise direction through the points p_i the fitness error of the approximation of the piece of the curve from the point p_0 to p_i is calculated. If the error exceeds a certain threshold the current curve point p_i is declared as the polygon vertex and the same procedure is repeated starting from this point until the entire curve is spanned. The primary disadvantage of the merge method is that polygon vertexes do not coincide with curve inflection points. The *splitting technique* avoids this problem. In order to start splitting of the curve two curve inflection points must be found which can be, for example, the points of maximal curvature. Than the curve segment between these points is recursively divided into sub-segments until the fitness errors of all sub-segments are below a certain threshold. A point on that part of the curve which is approximated by a straight line interval, l_j, is chosen to be a new vertex of the polygonal approximation if 1) the fitness error for the current approximation by l_j of the considered piece of the curve is larger than the predefined value and 2) the distance from this point to the approximation line l_j is maximal.

3) The third method is related to the *intrinsic equation* of a curve. The points of maximal curvature of the curve serve as the vertexes of the polygon which approximates the curve (Fig. 2.1.12).

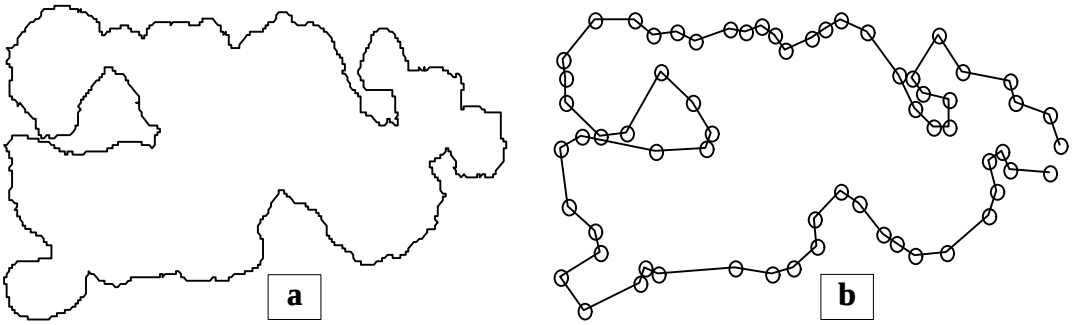

Fig. 2.1.12. Polygonal approximation: **a)** the contour of a figure; **b)** the same contour approximated by a polygon using the points of maximal curvature.

Fourier analysis of contour functions

Fourier analysis [2.1.1-2.1.8, 2.1.16-2.1.23] is one of the most frequently used methods in shape analysis. Consider a periodic piecewise continuous and differentiable function $f(x)$ defined on $\lfloor 0,\ 2\pi \rfloor$ which can be one of contour functions introduced above. Such function can be approximated by a *Fourier series*:

$$f(x) = \frac{a_0}{2} + \sum_{k=1}^{\infty} \left(a_k \cos kx + b_k \sin kx \right)$$

where the *Fourier coefficients* are

$$a_k = \frac{1}{\pi} \int_{-\pi}^{\pi} f(x) \cos kx \, dx \text{ and } b_k = \frac{1}{\pi} \int_{-\pi}^{\pi} f(x) \sin kx \, dx .$$

The Fourier series can be also written as

$$f(x) = \frac{a_0}{2} + \sum_{k=1}^{\infty} A_k \sin\left(kx + \varphi_k \right)$$

where $A_k = \sqrt{a_k^2 + b_k^2}$ and $tg\varphi_k = a_k / b_k$, or in complex form as

$$f(x) = \sum_{k=-\infty}^{\infty} c_k e^{ikx} \text{ where } c_k = \frac{1}{2\pi} \int_{-\pi}^{\pi} f(x) e^{-ikx} dx = \begin{cases} \frac{a_0}{2} & if \quad k = 0 \\ \frac{1}{2}\left(a_k - ib_k \right) & if \quad k > 0 \\ \frac{1}{2}\left(a_{-k} + ib_{-k} \right) & if \quad k < 0 \end{cases} .$$

Each term of the Fourier series is called *harmonic* and A_k is the *harmonic amplitude*. The sequence $\{A_k\}$ is called the *amplitude spectrum*.

Some general properties of Fourier series expansion and Fourier coefficients are given below.

1. The coefficient a_0 equals to the mean value $\bar{f}$ of $f(x)$.
2. The Fourier coefficients depend in different ways on the form of the function: the a_k, b_k and A_k for small k tend mainly to describe the global characteristics, while the coefficients for large k describe roughness;
3. Symmetry properties of the figure are reflected by the Fourier coefficients. That is, if the function $f(x)$ have a smaller period than 2π, namely $2\pi / l$, where $l \in \mathrm{N}$ and $l > 1$, then if a_0 is excluded, only the coefficients a_k and b_k with $k = lm$ where $m = 1, 2, \ldots$ differ from zero.
4. The operation that assigns to a function $f(x)$ its Fourier coefficients a_k and b_k is linear. That is, let $f(x)$ be given in the form

   $$f(x) = \sum_{i=1}^{m} \gamma_i f_i(x)$$

   and let $a_k^{(i)}$ and $b_k^{(i)}$ be the Fourier coefficients of the functions $f_i(x)$, then the Fourier coefficients of $f(x)$ can be written as

   $$a_k = \sum_{i=1}^{m} \gamma_i a_k^{(i)} \text{ and } b_k = \sum_{i=1}^{m} \gamma_i b_k^{(i)} .$$

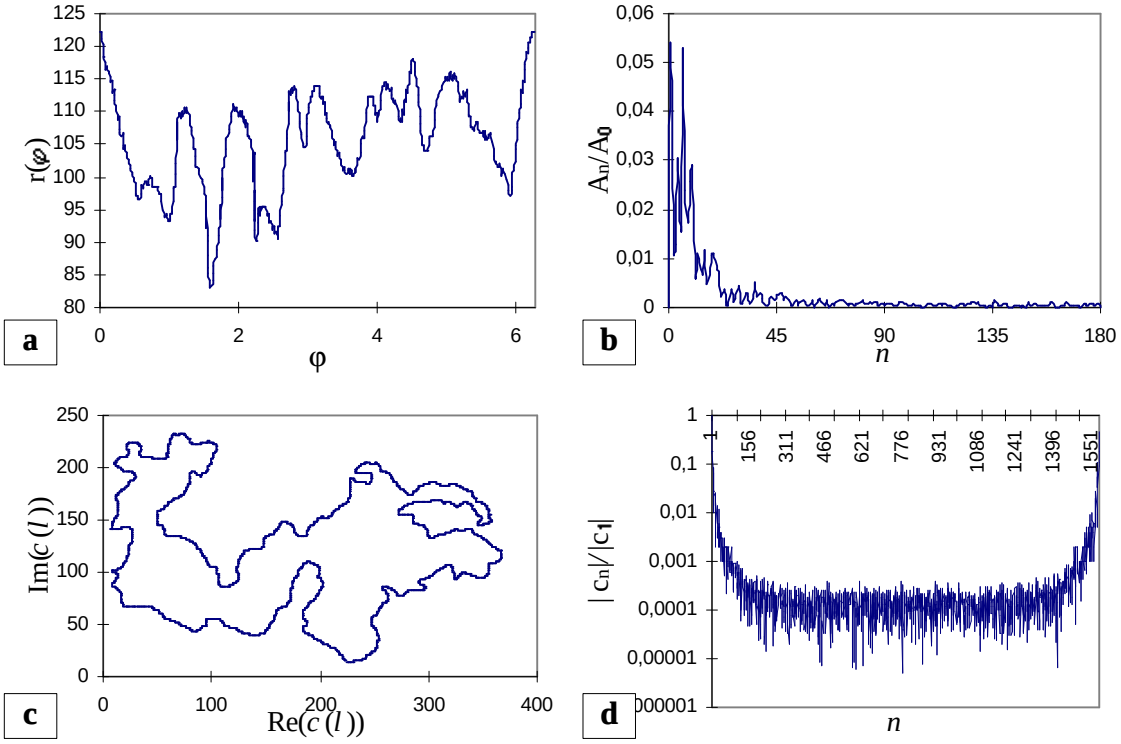

Fig. 2.1.13. a) a radius-vector function; **b)** normalized amplitude spectrum $\{A_n / A_0\}$ for the given radius-vector function; **c)** a contour complex function; **d)** normalized amplitude spectrum $\{|c_n|/|c_1|\}$ $(n \neq 0)$.

5. Several geometrical transformations of the contour of a figure are related to simple operations on the corresponding Fourier coefficients: if a translation of the contour has an influence on the contour function (e.g. the contour complex function) then the new Fourier coefficients remain the same except for $k = 0$; a shrinking or expanding the contour by a factor α results in scaling of the Fourier coefficients, $c'_k = \alpha c_k$ where c_k and c'_k are the Fourier coefficients of the original and scaled contours, respectively; changing the starting point in tracing the contour results in a modulation of the coefficients, $c'_k = c_k e^{-ikx_0}$ where x_0 is the new starting point; rotation of the contour by an angle θ_0 causes a constant phase shift of θ_0 in the Fourier coefficients, $c'_k = c_k e^{i\theta_0}$; finally reflection of the contour about a straight line $Ax + By + C = 0$ gives the new contour for which

$$c'_k = c^*_{-k} \frac{-(A+iB)^2}{A^2+B^2} + 2\delta_k \frac{-(A+iB)C}{A^2+B^2}.$$

6. The A_k (for all k) and $|c_k|$ (for all k except $k = 0$) are invariant with respect to shift of

the starting point (variable x), rotation and reflection of the contour. The quantities $c_k/|c_1|$, a_k/a_0, b_k/a_0 are invariant to scaling. Finally A_k/A_0 and $|c_k|/|c_1|$ are invariant to all above mentioned geometrical transformations. Examples of $\{A_k/A_0\}$ and $\{|c_k|/|c_1|\}$ for different contour functions are given in Fig. 2.1.13.

7. As in the theory of stochastic processes, there is a close connection between the contour covariance function $\chi_f(\varphi)$ and the Fourier coefficients A_k of a given function $f(x)$:

$$\chi_f(\varphi) = \frac{1}{2}\sum_{k=1}^{\infty} A_k^2 \cos k\varphi \text{ and } A_k^2 = \frac{2}{\pi}\int_0^{2\pi} \chi_f(\varphi)\cos k\varphi \, d\varphi \text{ where } A_0 = \bar{f}\,.$$

In the practice of shape analysis the discrete version of the Fourier transform is applied [2.1.1, 2.1.4]. Consider the value of the function $f(x)$ at N discrete equally spaced values of x_r (actually $x_r = 2\pi r/N$). Then the following equations can be written:

$$f(x_r) = a_0 + \sum_{n=1}^{[(N+1)/2]-1}\left(a_n \cos x_r n + b_n \sin x_r n\right),\; a_0 = \frac{1}{N}\sum_{r=0}^{N-1} f(x_r),$$

$$a_n = \frac{2}{N}\sum_{r=0}^{N-1} f(x_r)\cos x_r n \text{ and } b_n = \frac{2}{N}\sum_{r=0}^{N-1} f(x_r)\sin x_r n$$

where $r = 0, 1, \ldots, N-1$ and $n = 0, 1, \ldots, [(N+1)/2]-1$. Also

$$f(x_r) = \sum_{n=0}^{N-1} c_n e^{ix_r n} \text{ and } c_n = \frac{1}{N}\sum_{r=0}^{N-1} f(x_r) e^{-ix_r n}$$

where $r = 0, 1, \ldots, N-1$ and $n = 0, 1, \ldots, N-1$.

If a contour function $f(x)$ is approximated by an M-side polygon whose vertexes are known and are represented by points v_m where $m = 0, 1, \ldots, M-1$, simplified equations for the Fourier coefficients can be obtained [2.1.4, 2.1.8]:

$$a_0 = \pi - \frac{1}{L}\sum_{j=1}^{M} l_j \Delta\phi_j,\; a_m = \frac{-1}{m\pi}\sum_{j=1}^{M} \Delta\phi_j \sin\frac{2\pi m l_j}{L},$$

$$b_m = \frac{1}{m\pi}\sum_{j=1}^{M} \Delta\phi_j \cos\frac{2\pi m l_j}{L} \text{ and } c_m = \frac{L}{(2\pi m)^2}\sum_{j=1}^{M} \Delta\phi_j e^{\frac{-i2\pi m l_j}{L}}$$

where L is the length of the polygon, l_j is the arc length of j^{th} vertex from the starting point and $\Delta\phi_j$ is change of slope at the vertex j, that is

$$\Delta\phi_j = \frac{v_j - v_{j-1}}{|v_j - v_{j-1}|} - \frac{v_{j+1} - v_j}{|v_{j+1} - v_j|},\; l_j = \sum_{p=1}^{j} |v_p - v_{p-1}| \text{ for } m > 0 \text{ and } l_0 = 0\,.$$

In practice, Fourier analysis is applied in different ways depending of the contour function available. However, it is often enough to consider only the A_k/A_0 ($k = 1, 2, \ldots$) coefficients independently of what kind of contour function was analyzed, except, of course, in the case of complex contour function. Moreover, usually all necessary shape information is

accumulated in only the very few first coefficients.

When the contour of a figure is described by the radius-vector function $r_X(\varphi)$ the following structure, size and shape terms are often used.

The parameters for *global structure* and for *roughness* are

$$G_{n_1} = \sum_{n=1}^{n_1} A_n^2 \text{ and } R_{n_2,n_3} = \sum_{n=n_2}^{n_3} A_n^2$$

where n_1, n_2 and n_3 are suitable natural numbers chosen with the figures to be analyzed in mind. The *size term* is

$$R_0 = \sqrt{a_0^2 + \frac{1}{2}\sum_{n=1}^{[(N+1)/2]-1}\left(a_n^2 + b_n^2\right)} = \sqrt{A_0^2 + \frac{1}{2}\sum_{n=1}^{[(N+1)/2]-1} A_n^2}$$

where R_0 is called the *equivalent radius* and is the radius of a circle having the same area as that of the figure. In fact, the area of the figure may be stated in terms of the Fourier coefficients as $A(X) = \pi R_0^2$. The *shape terms* are

$$L_0 = \frac{a_0}{R_0} = \frac{A_0}{R_0},\ L_1(n) = 0,\ L_2(n) = \frac{\left(a_n^2 + b_n^2\right)}{2R_0^2} = \frac{A_n^2}{2R_0^2} \text{ and}$$

$$L_3(m,n) = \frac{3}{4R_0^3}\left(a_m a_n a_{n+m} - b_m b_n b_{n+m} + a_m b_n b_{n+m} + b_m a_n b_{n+m}\right) =$$

$$\frac{3}{4R_0^3}\left(A_m A_n A_{n+m}\cos\left(\varphi_{n+m} - \varphi_m - \varphi_n\right)\right)$$

where $n = 0, 1, \ldots, \left[(N+1)/2\right] - 1$ and $n + m = 2, 3, \ldots, \left[(N+1)/2\right] - 1$. The shape term L_0 is the size normalized mean radius of the figure's radial distribution, however the interpretation of other shape terms is not so simple. The quantity

$$L_2(n) \Big/ \sum_{j=1}^{[(N+1)/2]-1} L_2(j)$$

can be considered as a measure of the proportion of the radial variability of the figure that can be attributed to the n^{th} harmonic. The partial sum

$$\sum_{j=1}^{k} L_2(j)$$

can be used to describe how well the first k harmonics fit the observed radii. Actually, both parameters can be used not only for the Fourier analysis of the radius-vector function, but also when any other contour function is considered.

The size and shape terms are directly related to the mean μ_0, first μ_1, second μ_2 and third μ_3 moments about the mean of the figure's radial distribution:

$$\mu_0 = L_0 R_0 = a_0\,,\ \mu_1 = R_0 \sum_{n=1}^{[(N+1)/2]-1} L_1(n) = 0\,,\ \mu_2 = R_0^2 \sum_{n=1}^{[(N+1)/2]-1} L_2(n) \text{ and}$$

$$\mu_3 = R_0^3 \sum_{m=1}^{[(N+1)/2]-1} \sum_{n=1}^{[(N+1)/2]-1} L_3(m,n)\,.$$

A quantitative index of differences between different amplitude spectra may be obtained by determination of the average squared deviation of the radius-vector function from a circle of equal area. This '*roughness coefficient*' may be calculated as the square root of one-half the sum of the squared Fourier coefficients:

$$R' = \sqrt{\frac{1}{2} \sum_{n=1}^{[(N+1)/2]-1} \left(a_n^2 + b_n^2\right)} = \sqrt{\frac{1}{2} \sum_{n=1}^{[(N+1)/2]-1} A_n^2}\,.$$

Sometimes it is also convenient to consider a modified roughness coefficients spanning a selected range of harmonics rather than all of them:

$$R'_{n1,\,n2} = \sqrt{\frac{1}{2} \sum_{n=n_1}^{n_2} A_n^2}\,.$$

When the polar parametric function $\tau_X(t) = \left(d_X(t),\ \theta_X(t)\right)$ is considered the following Fourier analysis can be performed [2.1.18]. Fourier series expansions are used to represent $d_X^*(t)$ and $\theta_X^*(l)$. The equivalent radius is then defined as

$$R_0^2 = \frac{1}{2\pi} \int_0^{2\pi} \left(d^*(t)\right)^2 \theta^{*\prime}(t)\,dt\,.$$

The shape terms L_0, $L_2(n)$ and $L_3(m,n)$ for the $d_X^*(t)$ and $\theta_X^*(l)$ expansions are defined in a similar way as described for the radius-vector function.

For the case of the contour complex function $c_X^*(t)$ the information useful for shape characterization is accumulated in $|c_k|/|c_1|$ [2.1.4-2.1.7]. The coefficient c_0 is usually not used because it reflects the contour position.

Some other possible series expansions of contour functions

Not only the Fourier series expansion of a function can be performed, there are some other series expansions [2.1.4, 2.1.24] which can be useful in shape analysis. Before introducing them some general ideas of function series expansions will be given.

For continuous functions, orthogonal series expansions provide series coefficients which can be used for any further processing or analysis of the functions. For a one-dimensional function $f(x_r)$ given at N equally spaced points x_r, a unitary transformation is written as

$$u_n = \sum_{r=0}^{N-1} f(x_r) a^*_{r,n} \text{ where } f(x_r) = \sum_{n=0}^{N-1} u_n a_{r,n} .$$

This can be also written in matrix form as $\mathbf{u} = \mathbf{Af}$ where $\mathbf{A}^{-1} = \mathbf{A}^{*\mathrm{T}}$. This gives $\mathbf{f} = \mathbf{A}^{*\mathrm{T}}\mathbf{u}$ where the columns of $\mathbf{A}^{*\mathrm{T}}$, that is, the vectors $\mathbf{a}^*_r = \left\{a^*_{r,n},\ 0 \le n \le N-1\right\}^{\mathrm{T}}$ are called the *basis vectors* of $\mathbf{A}$. The series coefficients u_n give a representation of the function $f(x_r)$.

The *one-dimensional discrete cosine series expansion* of a function $f(x_r)$ given at N equally spaced points x_r, is defined as

$$f(x_r) = \sum_{n=0}^{N-1} \alpha_n u_n \cos\frac{\pi(2n+1)r}{2N}$$

where $\alpha_n = \sqrt{2/N}$, $\alpha_0 = \sqrt{1/N}$ and

$$u_n = \alpha_n \sum_{r=0}^{N-1} f(x_r) \cos\frac{\pi(2n+1)r}{2N} .$$

The *one-dimensional discrete sine series expansion* of a function $f(x_r)$ given at N equally spaced points x_r ($x_r = 2\pi r/N$), is defined as

$$f(x_r) = \sqrt{\frac{2}{N+1}} \sum_{n=0}^{N-1} u_n \sin\frac{\pi(r+1)(n+1)}{N+1}$$

where

$$u_n = \sqrt{\frac{2}{N+1}} \sum_{r=0}^{N-1} f(x_r) \sin\frac{\pi(r+1)(n+1)}{N+1} .$$

The *one-dimensional discrete Walsh-Hadamard series expansion* of a function $f(x_r)$ given at N ($N = 2^n$) equally spaced points x_r, is defined as

$$f(x_r) = \frac{1}{\sqrt{N}} \sum_{m=0}^{N-1} u_m (-1)^{b(r,m)}$$

where

$$b(r,\ m) = \sum_{i=0}^{n-1} r_i m_i \quad (r_i,\ m_i = 0, 1)$$

and $\{r_i\}$, $\{m_i\}$ are the binary representations of r and m, that is

$$r = r_0 + 2r_1 + \quad \ldots \quad + 2^{n-1} r_{n-1} \text{ and } m = m_0 + 2m_1 + \quad \ldots \quad + 2^{n-1} m_{n-1} .$$

The Walsh-Hadamard coefficients are computed as

$$u_m = \frac{1}{\sqrt{N}} \sum_{r=0}^{N-1} f(x_r)(-1)^{b(r,m)} .$$

The *one-dimensional discrete Haar series expansion* of a function $f(x_r)$ given at N ($N = 2^n$) equally spaced points x_r, is presented as follows. The *Haar functions* $h_{p,q}(x)$ are defined on a continuous interval, $x \in [0,\ 1]$, as

$$h_{0,0}(x) = \frac{1}{\sqrt{N}} \text{ and } h_{p,q}(x) = \frac{1}{\sqrt{N}} \begin{cases} 2^{p/2}, & \frac{q-1}{2^p} \le x < \frac{q-1/2}{2^p} \\ -2^{p/2}, & \frac{q-1/2}{2^p} \le x < \frac{q}{2^p} \\ 0, & \textit{otherwise} \end{cases} .$$

The Haar transform is obtained by re-scaling of x_r ($x'_r = g(x_r)$) in such a way that $x'_r \in [0,\ 1]$ and applying the matrix form of a unitary transform for $f(x'_r)$ and $h_{p,q}(x)$.

The *one-dimensional Gabor series expansion* of a function $f(x)$ is defined based on the short-time Fourier transform:

$$u_{\varpi,\tau} = \int_{-\infty}^{\infty} g^*(t-\tau) u_t e^{-i2\pi\omega t} dt = e^{-i2\pi\omega t} \int_{-\infty}^{\infty} \hat{g}^*(\nu - \varpi) \hat{u}_\nu e^{i2\pi\nu\tau} d\nu$$

where $\hat{u}_\nu$ and $\hat{g}$ denote the Fourier transforms of u_t and g, respectively, * denotes the complex conjugate and the window is a Gaussian:

$$\hat{g}(\mu) = \frac{1}{\sigma\sqrt{2\pi}} e^{\frac{-\mu^2}{2\sigma^2}} .$$

Some other series expansions of the contour functions are reported in the literature including *KL*, *Slant*, *sinusoidal*, *singular value decomposition* series expansions [2.1.4], etc. However, we have never seen in the literature any examples of their application for the shape analysis.

Ones a contour function is represented by series coefficients, different methods can be employed for the extraction of meaningful information from this representation. Of course, choosing a particular method depends on many factors and can be hardly standardized. However, one common way for analyzing series coefficients is through the identification and characterization of a few maximal coefficients. Another possible method of analysis is based on the idea that the same series coefficients for the same contour functions of different figures mean the same things and, therefore, can be compared. For the Gabor series expansion two other methods can be employed. The response of the transform for different parameters ω and τ can be used for the analysis. Also the projection of the response onto box axes generates images which can reveal essential features of the analyzed contour functions.

Multiscale shape analysis using continuous wavelet transform

Consider a contour function $f(x)$. Its *continuous wavelet transform* [2.1.25-2.1.28] with respect to a wavelet mother function $\psi(x)$ is defined as

$$U(a,\ b) = \int_{-\infty}^{\infty} f(x)\psi_{(a,\ b)}(x)dx$$

where the wavelets used are of the form of Grossmann-Morlet wavelets:

$$\psi_{(a,\ b)}(x) = \frac{1}{\sqrt{a}}\psi\left(\frac{x-b}{a}\right) \text{ where } a > 0,\ b \in \mathrm{R}.$$

Wavelets are functions $\psi\colon \mathrm{R} \to \mathrm{R}$ with the property that $\{\psi_{(a,\ b)}\}$ forms an orthonormal basis of $L^2(\mathrm{R})$. Some examples of the Daubechies family of mother wavelets are given in Fig. 2.1.14.

Basically, wavelet transform of a function $f(x)$ is the set of coefficients $U(a,\ b)$ (Fig. 2.1.15a). Behavior of the coefficients under basic geometrical transformation of the analyzed figure can be predicted as:

1) under *translation*: $U[\psi;\ f(x)+z] = U[\psi;\ f(x)] + U[\psi;\ z] = U[\psi;\ f(x)]$;

2) under *scaling*: $U[\psi;\ cf(x/c)](a,\ b) = cU[\psi;\ f(x)](a/c,\ b/c)$;

3) under *rotation*: $U[\psi;\ e^{i\theta} f(x-x_0)](a,\ b) = e^{i\theta}U[\psi;\ f(x)](a,\ b-x_0)$

where $f(x)$, in general case, is a complex function, $U[\psi;\ f(x)](a,\ b) \equiv U(a,\ b)$, $z \in \mathrm{C}$, $c \in \mathrm{R}^+$, $x_0 \in \mathrm{R}$ and $\theta \in [0,\ 2\pi]$. If a wavelet with compact support is used, then local modifications of the shape affect only locally the wavelet representation. This property is particularly important when partial occlusion occurs.

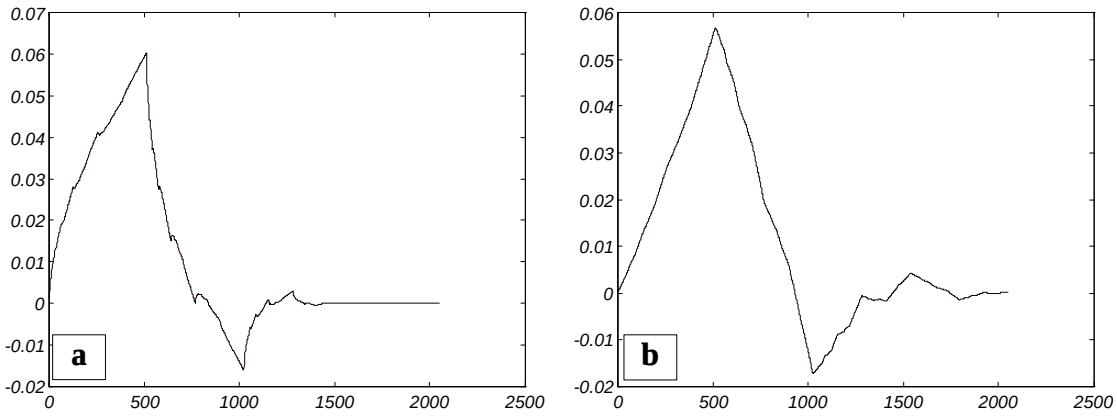

Fig. 2.1.14. Examples of mother wavelets: **a)** the Daubechies-4 wavelet basic function; **b)** the Daubechies-6 wavelet basic function.

Different shape properties can be obtained from the wavelet representation. The basic idea of such shape analysis is to find the vertical maxima lines of the wavelet representation. The

set of all vertical maxima lines is called the *skeleton* of the wavelet representation (Fig. 2.1.15b). The scale-space lifetime of each maxima line or, alternatively, their length can be used as a measure of their relevance. Most relevant maxima lines correspond to the dominant points (corners) on the analyzed contour.

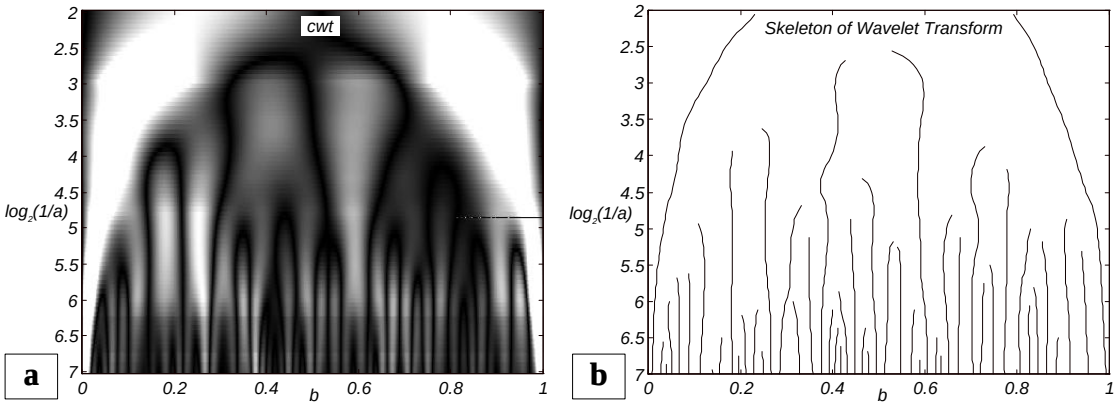

Fig. 2.1.15. Wavelet analysis: **a)** continuous wavelet transform (using 'Sombrero' wavelets) of the normalized tangent-angle function $\tilde{\phi}_X(t)$ shown in Fig. 2.1.10b; **b)** skeleton of the wavelet transform. Calculations were performed by MatLab using WaveLab package [2.1.29].

Another interesting application of wavelet representation is the analysis of natural scales of a contour. Such analysis can be hardly carried out by standard methods of curvature analysis because the perceived patterns on the contour can be characterized not only in terms of local features, but also by more global ones such as the organization of the local features, their periodicity, modulations, etc. The natural scale can be characterized by searching the horizontal maxima lines.

Fractal analysis is another example of what can be done using wavelet representation of the contour function. For this purpose the contour complex function $z_X(l) = x_X(l) + iy_X(l)$ should be used. Of course, the corresponding wavelet transform coefficients $U(p_1,\ p_2)$ will be also complex and their modules $|U(p_1,\ p_2)|$ should be used for the fractal analysis.

Shape curvature scale space representation

A curvature scale space representation [2.1.30-2.1.33] is a multi-scale organization of the invariant geometrical features such as the curvature zero-crossing points of a planar curve (actually, only closed contours will be considered here). To compute it the contour parametric function $c_X(l)$ and the contour curvature function $\kappa_X(l)$ are used. The *evolved*

version of the contour C is defined as $C_\sigma = \left(X\left(l,\ \sigma\right),\ Y\left(l,\ \sigma\right)\right)$ where

$$X\left(l,\ \sigma\right) = x(l) \otimes g\left(l,\ \sigma\right),\ Y\left(l,\ \sigma\right) = y(l) \otimes g\left(l,\ \sigma\right),$$

$\otimes$ is the convolution operator and $g\left(l,\ \sigma\right)$ denotes a one-dimensional Gaussian kernel of width σ :

$$g\left(l,\ \sigma\right) = \frac{1}{\sigma\sqrt{2\pi}} e^{\frac{-l^2}{2\sigma^2}}.$$

The convolution is defined as

$$F\left(l,\ \sigma\right) = f\left(l\right) \otimes g\left(l,\ \sigma\right) = \int_{-\infty}^{\infty} f\left(s\right) \frac{1}{\sigma\sqrt{2\pi}} e^{\frac{-(l-s)^2}{2\sigma^2}} ds \approx \sum_{s=-3\sigma}^{3\sigma} f\left(l+s\right) \frac{1}{\sigma\sqrt{2\pi}} e^{\frac{-(l-s)^2}{2\sigma^2}}.$$

Then the curvature function $\kappa(l)$ for the evolved contour C_σ is calculated as

$$\kappa\left(l,\ \sigma\right) = \frac{X'\left(l,\ \sigma\right)Y''\left(l,\ \sigma\right) - X''\left(l,\ \sigma\right)Y'\left(l,\ \sigma\right)}{\left(X'^2\left(l,\ \sigma\right) + Y'^2\left(l,\ \sigma\right)\right)^{3/2}}.$$

The process of generation the ordered sequence of evolved contours from a contour C is called the *evolution* of the contour C. The function defined implicitly by $\kappa\left(l,\ \sigma\right) = 0$ is the *curvature scale space image* (cssi) of C. It can be represented graphically as a binary image (Fig. 2.1.16b) in which each row corresponds to a specific value of σ and each column to a specific value of l. Often the normalized arc length parameter which is defined on $[0, 1]$, is used instead of l.

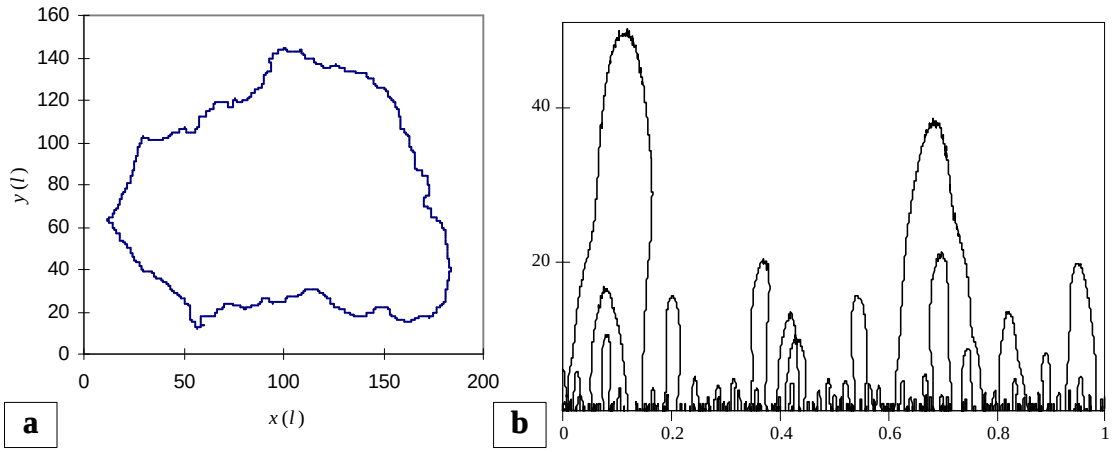

Fig. 2.1.16. a) the contour of a figure; **b)** curvature scale space image of the contour. Calculations were performed by MathCAD.

The curvature scale space image of a contour is a convenient shape representation which can be useful for such problems as shape recognition and matching, overlapping objects shape

extraction, etc. This representation is invariant under figure translation. Size changes of analyzed figure result in re-sizing of the corresponding cssi in the vertical direction, rotation itself of the figure changes nothing, but change of the starting point causes a circular shift of the corresponding cssi in horizontal direction whereas reflection of the figure results in reflection of its cssi. The method is robust to noise, small distortions on the contour do not change corresponding cssi too much.

2.2. Set theory approach

A large variety of methods of treating a figure in the sense of the set theory and mathematical morphology are available. The simplest methods are based on obtaining different geometrical shape rations as discussed below. If the aim is discrimination and classification, the use of shape ratio is frequently equivalent to or even more effective than more complicated methods. As an alternative to the contour functions it is possible to introduce some other functions describing different figure properties. Of particular interest are the chord length distribution function and the spherical erosion function. Also some ideas of the theory of random sets can be used for form statistics. Finally, sets (figures) can be considered in the sense of fractal geometry as described below.

2.2.1. Simple geometrical shape parameters

There are many shape ratios describing certain geometrical properties. The following figure parameters [2.2.1.-2.2.11] are often used (Fig. 2.2.1):

- $A(X)$ is the area of the figure X;
- $P(X)$ is the perimeter of the figure X;
- $D_A(X)$ and $D_P(X)$ are the diameters of circles with area $A(X)$ and with perimeter $P(X)$, respectively: $D_A(X) = 2\sqrt{A(X)/\pi}$ and $D_P(X) = P(X)/\pi$;
- $F_x(X)$, $F_y(X)$, $F_{\min}(X)$ and $F_{\max}(X)$ are the orthogonal projections of the figure X on the x and y axes and the minimal and the maximal orthogonal projections of the figure on a line, respectively, they also are known as Feret's diameters. In practice the maximal Feret's diameter is often used. It can be defined using coordinated of the contour of the figure X as

$$F_{\max}(X) = \sup\left\{\sqrt{(x_i - x_j)^2 + (y_i - y_j)^2} : \forall(x_i, y_i), (x_j, y_j) \in X\right\};$$

- $B(X)$ is the breadth of the figure X for a given direction; physically it is the same as, for example, $F_x(X)$ for a given orientation of the figure X;

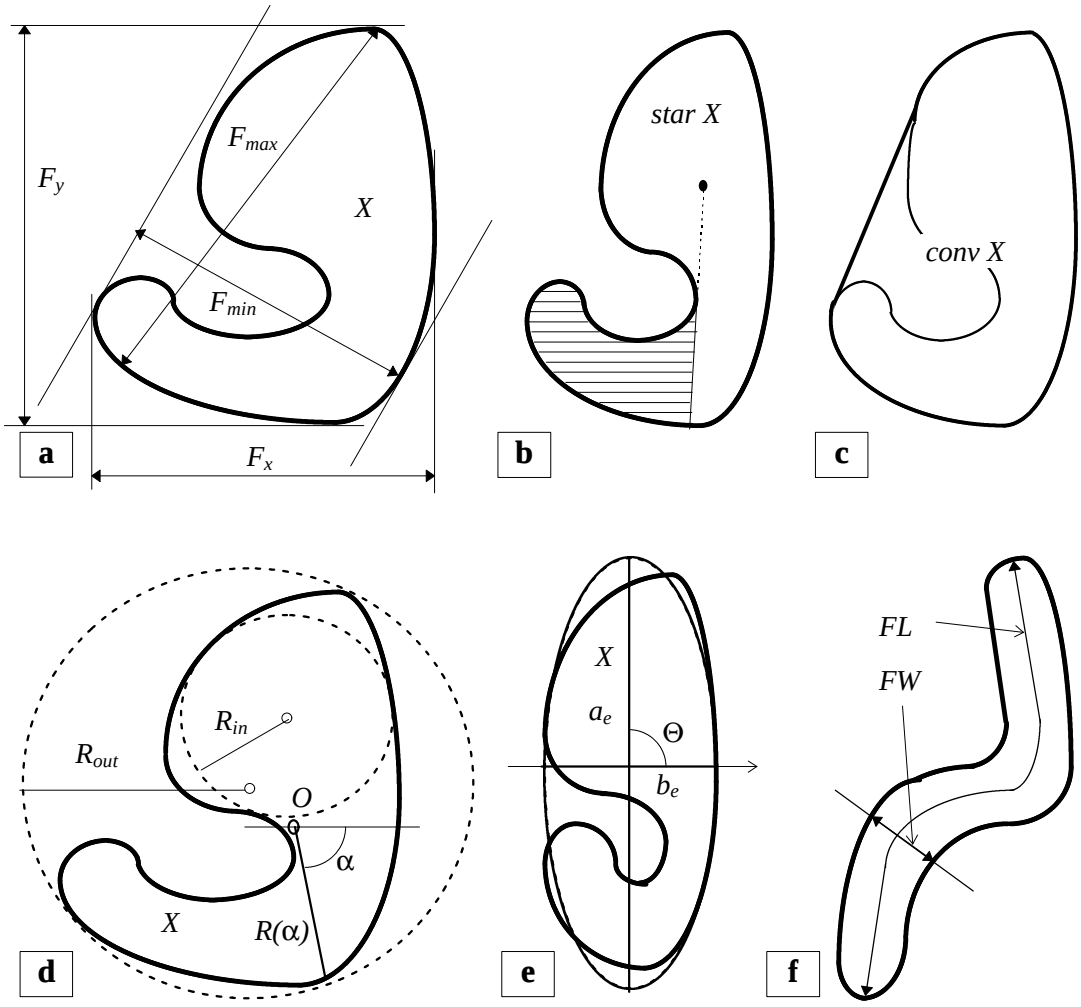

Fig. 2.2.1. Examples of different geometrical parameters: **a)** Feret's diameters; **b)** definition of the 'star' of the figure; the non-shaded part of the figure is visible from O and forms the star with respect to O; **c)** the convex hull for the given figure; **d)** the largest disc in X and the smallest disc which completely includes X; $R(\alpha)$ is the distance from the center of gravity O of the figure X to its boundary point in a given direction α; **e)** $a_e(X)$ and $b_e(X)$ are the lengths of the long and short semi-axes of the ellipse with area $A(X)$ and perimeter $P(X)$; **f)** fiber length and fiber width.

- $MD(X)$ is Martin's diameter - the distance between opposite sides of the figure X measured crosswise of the figure and on a line bisecting the figure's area; $MD_x(X)$ and

$MD_y(X)$ are Martin's diameters for horizontal and vertical directions, respectively;

- $S(X)$ is the so-called 'central symmetrization' of the figure X: $S(X) = 1/2\left(X \oplus \breve{X}\right)$ where $\breve{X}$ is the set reflected at the origin, $\breve{X} = \left\{x\colon -x \in X\right\}$;
- *conv* X is the convex hull of X;
- *star* X is the part of X seen from a random point in X; particularly, this parameter is useful when physically important point in the figure X is chosen to be the origin point;
- $R_{in}(X)$ and $R_{out}(X)$ are the radii of the largest disc in X and the smallest disc which completely includes X;
- $R(X)$ is the distance from an origin point in the figure X to its boundary point for a given direction; $\overline{R}(X)$ is the average distance for all possible directions for a given point; particularly, this parameter is useful when a physically important point in the figure X is chosen to be the origin point;
- $a_e(X)$ and $b_e(X)$ are the lengths of the long and short semi-axes of the ellipse with area $A(X)$ and perimeter $P(X)$:

$$a_e(X) = \alpha(X) + \sqrt{\left(\alpha(X)\right)^2 - A(X)/\pi}\,,\ b_e(X) = A(X)\Big/\left(\pi a_e(X)\right) \text{ where}$$
$$\alpha(X) = \frac{1}{3}\left(\sqrt{A(X)/\pi} + P(X)/\pi\right);$$

- $a_r(X)$ and $b_r(X)$ are the lengths of the long and short semi-axes of the radial-rhombus of area $A(X)$ and mean radius-vector $\overline{R}(X)$:

$$a_r(X) = \overline{R}(X) + \sqrt{3}\sigma\left(R(X)\right),\ b_r(X) = \overline{R}(X) - \sqrt{3}\sigma\left(R(X)\right) \text{ where}$$
$$\sigma\left(R(X)\right) = \sqrt{A(X)/\pi - \left(\overline{R}(X)\right)^2}\,;$$

- $FL(X)$ and $FW(X)$ are the fiber length and fiber width of the figure X;
- $\bar{x}(X)$ and $\bar{y}(X)$ are the coordinates of the center of gravity (also called center of mass or centroid); they are determined just by averaging the coordinates of each point of the figure X as

$$\bar{x}(X) = \sum_{i,\,j:\left(x_i,\,y_j\right)\in X} x_i \Big/ A(X) \text{ and } \bar{y}(X) = \sum_{i,\,j:\left(x_i,\,y_j\right)\in X} y_j \Big/ A(X);$$

- Orientation of the figure can be characterized in terms of the moments about the x and y axes as

$$M_x(X) = \sum_{i,\,j:\left(x_i,\,y_j\right)\in X} x_i - \frac{\left(\sum_{i,\,j:\left(x_i,\,y_j\right)\in X} x_i\right)^2}{A(X)},\ M_y(X) = \sum_{i,\,j:\left(x_i,\,y_j\right)\in X} y_j - \frac{\left(\sum_{i,\,j:\left(x_i,\,y_j\right)\in X} y_j\right)^2}{A(X)} \text{ and}$$

$$M_{xy}(X) = \sum_{i,\, j:(x_i, y_j)\in X} x_i y_j - \left(\sum_{i,\, j:(x_i, y_j)\in X} x_i \sum_{i,\, j:(x_i, y_j)\in X} y_j \right) \Big/ A(X);$$

the angle of the minimum moment is

$$\Theta(X) = \tan^{-1}\left(\frac{\left(M_{xx}(X) - M_{yy}(X) + \sqrt{\left(M_{xx}(X) - M_{yy}(X)\right)^2 + 4\left(M_{xy}(X)\right)^2} \right)}{\left(2 M_{xy}(X)\right)} \right).$$

The following ratios [2.2.1-2.2.11] describe different shape properties (Fig. 2.2.2):

- The *area-perimeter ratio* (also known as *form factor* or *projection sphericity*) $4\pi A(X) \big/ \left(P(X)\right)^2$ characterizes deviations of the figure X from a circular form. For any disc it equals to 1 while for all other figures it is less than 1 - the smaller the ratio is, the greater the deviation from circular shape. The reciprocal of this expression is called the *circularity shape factor*. Sometimes this parameter is used in the form $1 - 4\pi A(X) \big/ \left(P(X)\right)^2$.
- *Wadell's circularity shape ratio* $D_A(X) / F_{\max}(X)$ is also equal to 1 for a disc, otherwise it is less than 1.
- *Drainage-basin circularity shape ratio* is $A(X) / D_P(X)$. It is equal to 1 for a disc, otherwise it is less than 1.
- Another Wadell's ratio which defines *degree of circularity*, is $2\sqrt{\pi A(X)} \big/ P(X)$. Actually, it is just the square root of the area-perimeter ratio. The reciprocal of this expression is the *Horton's compactness factor*.
- Another *Wadell's sphericity ratio* is $D_A(X) / D_{out}(X)$. A similar ratio is *Tickell's ratio* in the form $4A(X) \Big/ \left(\pi \left(D_{out}(X)\right)^2\right)$ which is, actually, squared Wadell's sphericity ratio.
- *Pentland's projection sphericity ratio* is $4A(X) \Big/ \left(\pi \left(F_{\max}(X)\right)^2\right)$.
- *Fischer's angularity ratios* are

  $$\sum_i \alpha_i(X) \Big/ 360^0 \text{ and } \sum_j \beta_j(X) \Big/ \sum_k \gamma_k(X)$$

  where $\alpha_i(X)$ are angels subtending noncurved parts of the contour of the figure X, $\beta_j(X)$ are angels subtending convex parts of the contour of the figure X and $\gamma_k(X)$ are angels subtending plane parts of the contour of the figure X .
- *Wadell's roundness factor* is

  $$\sum_{i=1}^{n} r_i(X) \Big/ \left(n R_{in}(X)\right)$$

  where r_i are the radii of the curvature at n points of large curvature on the contour of

X . For a disc it is 1, otherwise it is less than 1.

- *Pirard's roundness factor* is

$$1 \Big/ \sqrt{\sum_{i=1}^{n} \left(1 + R_{in}(X)/r_i(X)\right)^2 \Big/ (n-1)}$$

where r_i is the radius of the largest inscribed disc in the figure X crossing the i^{th} point of the contour of the X .

- *Wentworth's roundness ratio* is $4r(X)/\left(F_{\max}(X) + B(X)\right)$ where $r(X)$ is radius of the curvature of a most convex part of the contour of X and $B(X)$ is the breadth of X measured orthogonal to the line $F_{\max}(X)$.
- *Cailleux's roundness ratio* is $2r(X)/F_{\max}(X)$.
- The *rugosity coefficient* is defined as $P(X)/P(conv\ X)$.
- The *elongation factor* $B(X)/F_{\max}(X)$ where $B(X)$ is the breadth of X measured orthogonal to the line $F_{\max}(X)$, characterizes the elongation of the figure X .
- Another *elongation factor* is $F_{\min}(X)/B(X)$ where $B(X)$ is the breadth of X measured orthogonal to the line $F_{\min}(X)$.
- Yet another *elongation factor* is $FL(X)/FW(X)$.
- *Symmetry factor of Blaschke* is $1 - A(X)/A(S(X))$. It equals to 1 for symmetric convex figures, while, for example, for triangles it is $1/3$.

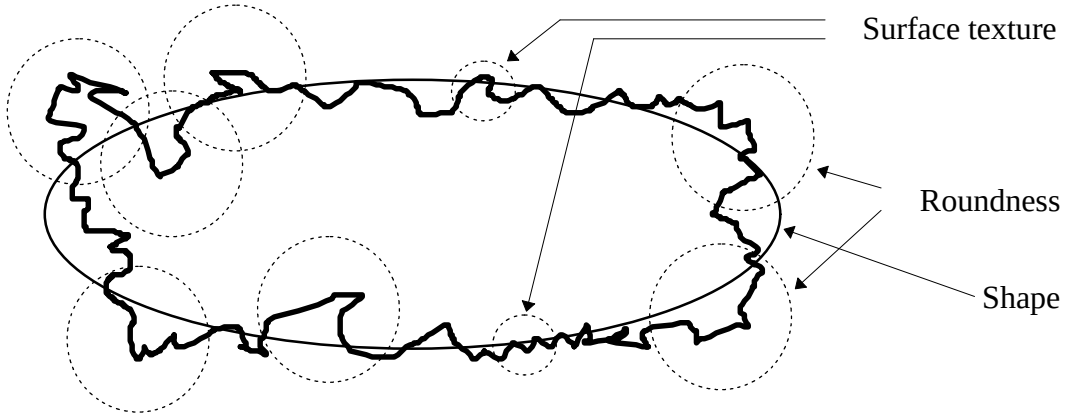

Fig. 2.2.2. Illustration of shape, texture and roundness of a figure.

- *Convexity ratio* (also known as *solidity*) $A(X)/A(conv\ X)$ characterizes deviations from convexity. Clearly, a convex figure X has the convexity factor 1, while in all other cases it is less than 1.

- Another *convexity ratio* $\left(A(X) - A(star\ X)\right)/\left(A(X)\right)$ also characterizes deviations from convexity. For convex sets it is zero, otherwise it is greater than zero.
- Yet another *convexity ratio* is $P(conv\ X)/P(X)$. For convex sets it is 1, otherwise it is less than 1.
- *Feret's ratio* (also known as an *aspect ratio*) is $F_{\min}(X)/F_{\max}(X)$. It characterizes dimensionality of the figure X.
- *Diameters ratios* are $MD_x(X)/F_x(X)$ and $MD_y(X)/F_y(X)$.
- The *radii ratio* (also known as *the inscribed circle sphericity*) is $R_{in}(X)/R_{out}(X)$.
- The *ellipse ratio* is $a_e(X)/b_e(X)$.
- The *radial-rhombus ratio* is $a_r(X)/b_r(X)$.
- The *modification ratio* is $R_{in}(X)/F_{\max}(X)$.
- The *extent ratio* is $A(X)/A\left(F_x(X)\times F_y(X)\right)$ where $F_x(X)\times F_y(X)$ is the bounding rectangle for a given figure X which is obtained by rotating the figure in such a way that $F_x(X) = F_{\min}(X)$.
- The *curl ratio* is $F_{\max}(X)/FL(X)$.
- *Medalia's dynamic shape factors* are defined as $K_a(X)/K_b(X)$ (*the anisometry*) and $4\pi K_a(X)K_b(X)/A(X)$ (*bulkiness*) where $K_a(X)$ and $K_b(X)$ are the radii of gyration about the central principal axes of the figure X.

2.2.2. Fractals in shape analysis

Application of fractal theory in shape analysis is one of the most rapidly developing modern directions in the field of shape analysis. The fractal dimension itself is often considered as a shape parameter describing different shape properties. There are a lot of examples of successful applications of this theory. However, there is a list of problems related to the methodology of the fractal dimension calculation. Thus, after brief introduction of the concept of fractal dimension, some of these problems will be discussed in Part 3.

Definition of fractal dimension

The Hausdorff-Besicovitch dimension [2.2.11-2.2.16] is defined as

$$\dim_H(X) = \inf\left\{\alpha:\ \ \alpha > 0,\ \ H_s^{\alpha}(X) = 0\right\} = \sup\left\{\alpha:\ \ \alpha > 0,\ \ H_s^{\alpha}(X) = \infty\right\}$$

where X is the analyzed figure and $H_s^{\alpha}(X)$ is the (spherical) α-dimensional Hausdorff

measure H^{α}:

$$H_s^{\alpha}(X) = \omega_{\alpha} \lim_{\delta \to 0} \inf \left\{ \sum_i r_i^{\alpha} : \quad X \subset \bigcup_i b(x_i, r_i), \quad r_i < \delta \right\}.$$

Here ω_{α} denotes the volume of the unit sphere in R^{α} for integer α. The last equation has the following meaning. The volume $\omega_0 r_0^{\alpha} + \omega_1 r_1^{\alpha} + \ldots$ of the figure X is found covering X by closed discs $b(x_i, r_i)$ with radii smaller than a given positive number δ. Of course, there are many such coverings; that is, there is freedom in choosing x_i and r_i. But the definition of $H_s^{\alpha}(X)$ requires that the smallest value of $\omega_0 r_0^{\alpha} + \omega_1 r_1^{\alpha} + \ldots$ is obtained which is denoted by $S_{\delta}^{\alpha}(X)$ and $H_s^{\alpha}(X) = \lim_{\delta \to 0} S_{\delta}^{\alpha}(X)$. For elementary X, in the case $\alpha = 1$ and $\alpha = 2$, $S_{\delta}^{\alpha}(X)$ yields the length and area of X, respectively.

In practice, however, such notation of Fractal dimension can be hardly used to determine the fractal properties of boundaries of objects. Fortunately, there are some other definitions of fractal dimension from which practical methods of fractal dimension calculation can be derived. For example, the notation of fractal dimension as packing dimension [2.2.11, 2.2.13, 2.2.16] in the following form is widely used. Consider the lower and upper Minkowski-Bouligand dimension $\dim_{M_*}(X)$, $\dim_{M^*}(X)$. Actually, because a general inequality is $\dim_{M^*}(X) \geq \dim_{M_*}(X) \geq \dim_H(X)$, only the notation of the lower Minkowski-Bouligand dimension will be used:

$$\dim_{M_*}(X) = \inf\{\alpha: \quad \alpha > 0, \quad M_*^{\alpha}(X) = 0\} = \sup\{\alpha: \quad \alpha > 0, \quad M_*^{\alpha}(X) = \infty\}$$

where the lower α-dimensional Minkowski content $M_*^{\alpha}(X)$ is defined as

$$M_*^{\alpha}(X) = \lim_{r \to 0} \inf \frac{A(X_r)}{r^{2-\alpha} \omega_{2-\alpha}}.$$

It has the following meaning. Let B be a smooth curve of length $l(B)$. The outer parallel set $B_r = B \oplus b(0, r)$ is formed where $\oplus$ is the Minkowski addition operation. For small r the area of B_r equals to $2rl(B)$, so it can be calculated as

$$l(B) = \lim_{r \to 0} \frac{A(B_r)}{2r}$$

where $A(B_r)$ is the area of the set B_r. In the case of a 'rough' curve this limit does not necessarily exist. Therefore corresponding infima and suprema are considered, which yield for B 'lower' and 'upper' lengths:

$$l_*(B) = \lim_{r \to 0} \inf \frac{A(B_r)}{2r} \text{ and } l^*(B) = \lim_{r \to 0} \sup \frac{A(B_r)}{2r}.$$

By introducing a positive real number α $(0 < \alpha \leq 2)$ the lower (upper) α-dimensional Minkowski content $M_*^{\alpha}(X)$ is obtained.

The following formula can be used to calculate the lower Minkowski-Bouligand dimension:

$$\dim_{M*}(B) = 2 - \lim_{r\to 0} \sup \frac{\log A(B_r)}{\log r}.$$

The method, which is based on direct application of this formula, is called 'Minkowski sausage' method. There are some other important formulae which can be used to calculate fractal dimension:

$$\dim_{M*}(B) = -\lim_{r\to 0} \sup \frac{\log M_r(B)}{\log r} \text{ and } \dim_{M*}(B) = -\lim_{r\to 0} \sup \frac{\log Q_r(B)}{\log r}$$

where $M_r(B)$ is the maximal number of open discs of radius r and centre in B that do not overlap; $Q_r(B)$ is the number of squares containing points of B. First equation is directly related to 'hand and dividers' method which will be discussed later, and the last equation is related to box-counting method.

References

[2.1.1] D. Stoyan and H. Stoyan, *Fractals, Random Shapes and Point Fields (Methods of Geometrical Statistics)*, John Wiley & Sons, Chichester, 1995.

[2.1.2] B. Raeymaekers, P. Van Espen and F. Adams, The morphological characterization of particles by automated scanning electron microscopy, Microchimica Acta, vol. 2, pp. 437-454, 1984.

[2.1.3] D. Luerkens, J. Beddow and A. Vetter, *Morphological Fourier descriptors*, Powder Technology, vol. 31, pp. 209-215, 1982.

[2.1.4] A. Jain, *Fundamentals of Digital Image Processing*, Prentice-Hall International, Englewood Cliffs, 1989.

[2.1.5] V. Kindratenko and P. Van Espen, *Classification of irregularly shaped micro-objects using complex Fourier descriptors*, Proceedings of 13th ICPR, vol. II, pp. 285-289, 1996.

[2.1.6] M. Thomas, R. Wiltshire and A. Williams, *The use of Fourier descriptors in the classification of particle shape*, Sedimentology, vol. 42, pp. 635-645, 1995.

[2.1.7] T. Wallace and P. Wintz, *An effective three-dimensional aircraft recognition algorithms using normalized Fourier descriptors*, Computer Graphics and Image Processing, vol. 13, pp. 99-126, 1980.

[2.1.8] S. Fong, J. Beddow and A. Vetter, *A refined method of particle shape representation*, Powder Technology, vol. 22, pp. 17-21, 1979.

[2.1.9] M. Worring, *Shape Analysis of Digital Curves*, Febodruk, Enschede, 1993.

[2.1.10] W. Dahmen, M. Gasca and C. Micchelli, eds, *Computation of Curves and Surfaces*, NATO ASI Series, Series C: Mathematical and Physical Sciences, vol. 307, Kluwer Academic Publishers, Dordrecht, 1990.

[2.1.11] R. Cesar Jr. and L. Costa, *Shape characterization in natural scales by using the multiscale bending energy*, Proceedings of 13th ICPR, vol. I, pp. 735-739, 1996.

[2.1.12] R. Cesar Jr. and L. Costa, *Piecewise linear segmentation of digital contours in 0(N.Log(N)) through a technique based on effective digital curvature estimation*, Real-Time Imaging, vol. 1, pp. 409-417, 1995.

[2.1.13] B. Li and S. Ma, *Unbiased and consistent estimation of moment difference*, Technical Report, National Pattern Recognition Laboratory, Institute of Automation, Chinese Academy of Sciences, 1994.

[2.1.14] G. Lambert and H. Gao, *Line moments and invariants for real time processing of vectorized contour data*, Lecture Notes in Computer Science, vol. 974, pp. 347-352, Springer-Verlag, Berlin, 1995.

[2.1.15] G. Lambert and J. Noll, *Discrimination properties of invariants using the line moments of vectiruzed contours*, Proceedings of 13th ICPR, vol. II, pp. 735-739, 1996.

[2.1.16] R. Duda and P. Hart, *Pattern Classification and Shape Analysis*, Wiley, New York, 1973.

[2.1.17] J. Beddow, ed., *Advanced Particulate Morphology*, Series in Fine Particle Science and Technology, vol. 1, CRC Press, Boca Raton, 1980.

[2.1.18] J. Beddow, ed., *Particle Characterization in Technology*, vol. II: *Morphological Analysis*, CRC Press, Boca Raton, 1984.

[2.1.19] J. Marshall, ed., *Clastic Particles: Scanning Electron Microscopy and Shape Analysis of Sedimentary and Volcanic Classes*, Van Nostrand Reinhold Company, New York, 1990.

[2.1.20] W. Full and R. Ehrlich, *Some approaches for location of centroids of quartz grain outlines to increase homology between Fourier amplitude spectra*, Mathematical Geology, vol. 14, no. 1, pp. 43-55, 1982.
[2.1.21] E. Derbyshire, D. Unwin, X. Fang and M. Langford, *The Fourier frequency-domain representation of sediment fabric anisotropy*, Computers and Geoscience, vol. 18, no. 1, pp. 63-73, 1992.
[2.1.22] R. Ehrlich and B. Weinberg, *An exact method for characterization of grain shape*, Journal of Sedimentology, vol. 40, no. 1, pp. 205-212, 1970.
[2.1.23] H. Bandemer, M. Albrecht and A. Kraut, *On using Fourier series in characterizing particle shape*, Particle Characterization, vol. 2, pp. 98-103, 1985.
[2.1.24] R. Cesar Jr. and L. Costa, *Shape characterization by using the Gabor transform*, Proceedings of 7th IEEE DSP Workshop, pp. 215-218, 1996.
[2.1.25] Y. Meyer, *Wavelets: Algorithms and Applications*, Society for Industrial and Applied Mathematics, Philadelphia, 1993.
[2.1.26] J. Antoine, D. Barache, R. Cesar Jr. and L. Costa, *Multiscale shape analysis using the continuous wavelet transform*, Proceedings of IEEE ICIP'96, pp. 101-105, 1996.
[2.1.27] Y. Nakamura, K. Satoda and M. Nagao, *Shape description and matching using wavelet extrema*, Proceedings of ACCV'93, pp. 640-643, 1993.
[2.1.28] B. Jawerth and W. Sweldens, *An overview of wavelet based multiresolution analyses*, SIAM Reviews, vol. 36, no. 3, pp. 377-412, 1994.
[2.1.29] WaveLab .701, URL: http://playfair.stanford.edu/~wavelab.
[2.1.30] F. Mokhtarian and A. Mackworth, *Scale-based description and recognition of planar curves and two-dimensional shapes*, IEEE Transactions on Pattern Analysis and Machine Intelligence, vol. PAMI-8, no. 1, pp. 34-43, 1986.
[2.1.31] A. Mackworth and F. Mokhtarian, *The renormalized curvature scale space and the evolution properties of planar curves*, Proceedings of CVPR'88, pp. 318-326, 1988.
[2.1.32] F. Mokhtarian and A. Mackworth, *A theory of multiscale, curvature-based shape representation for planar curves*, IEEE Transactions on Pattern Analysis and Machine Intelligence, vol. 14, no. 8, pp. 789-805, 1992.
[2.1.33] F. Mokhtarian, *Silhouette-based isolated object recognition through curvature scale space*, IEEE Transactions on Pattern Analysis and Machine Intelligence, vol. 17, no. 5, pp. 539-544, 1995.

[2.2.1] J. Russ, *The Image Processing Handbook*, 2nd edition, CRC Press, Boca Raton, 1995.
[2.2.2] A. Hawkins, *The Shape of Powder-Particle Outlines*, Research Studies Press, Chichester, 1993.
[2.2.3] W. Dahmen, M. Gasca and C. Micchelli, eds, *Computation of Curves and Surfaces*, NATO ASI Series, Series C: Mathematical and Physical Sciences, vol. 307, Kluwer Academic Publishers, Dordrecht, 1990.
[2.2.4] J. Beddow, ed., *Particle Characterization in Technology*, vol. II: *Morphological Analysis*, CRC Press, Boca Raton, 1984.
[2.2.5] A. Medalia, *Dynamic shape factors of particles*, Powder Technology, vol. 4, pp. 117-138, 1970/71.
[2.2.6] R. Reyment, *Multivariate morphometrics and analysis of shape*, Mathematical Geology, vol. 17, no. 6, pp. 591-609, 1985.

[2.2.7] S. Drescher, E. Heidenreich and G. Müller, *Technologically relevant particle shape analysis*, Particles and Particle System Characterization, vol. 7, pp. 30-35, 1990.

[2.2.8] D. Benn and C. Ballantyne, *The description and representation of particle shape*, Earth Surface Processes and Landforms, vol. 18, pp. 665-672, 1993.

[2.2.9] E. Pirard, *Shape processing and analysis using the calypter*, Journal of Microscopy, vol. 175, pp. 214-221, 1994.

[2.2.10] E. Pirard, *Roughness analysis on powders using mathematical morphology*, Acta Stereologica, vol. 11, suppl. 1, pp. 533-538, 1992.

[2.2.11] D. Stoyan, H. Stoyan, *Fractals, Random Shapes and Point Fields (Methods of Geometrical Statistics)*, John Wiley & Sons, Chichester, 1995.

[2.2.12] K. Falconer, *The Geometry of Fractal Sets*, Cambridge University Press, Cambridge, 1985.

[2.2.13] K. Falconer, *Fractal Geometry: Mathematical Foundations and Applications*, John Wiley & Sons, New York, 1990.

[2.2.14] B. Mandelbrot, *Fractals: Form, Chance and Dimension*, Freeman, San Francisco, 1977.

[2.2.15] J. Feder, *Fractals*, Plenum Press, New York, 1988.

[2.2.16] G. Cherbit, ed., *Fractals: Non-integer Dimensions and Applications*, Jonh Wiley & Sons, Chichester, 1991.